# Coastal hydrodynamics and anthropogenic activities drive mineralogical-geochemical spatial patterns and foraminiferal assemblages in the northern Gulf of St. Lawrence (eastern Canada)

Neha Joshi, Jean-Carlos Montero-Serrano, Vincent M.P. Bouchet, Emilie Arseneault, Émilie Saulnier-Talbot

Estuarine, Coastal and Shelf Science 335 (2026) 109828

Contents lists available at ScienceDirect

Estuarine, Coastal and Shelf Science

journal homepage: www.elsevier.com/locate/ecss

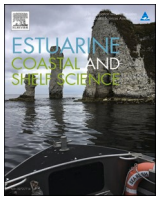

# Coastal hydrodynamics and anthropogenic activities drive mineralogical-geochemical spatial patterns and foraminiferal assemblages in the northern Gulf of St. Lawrence (eastern Canada)

Neha Joshi [a,b,*,1], Jean-Carlos Montero-Serrano [c,d], Vincent M.P. Bouchet [e], Emilie Arseneault [b,f], Émilie Saulnier-Talbot [a,b,f]

[a] Département de Géographie, Université Laval, Québec City, QC, Canada
[b] Institut de Biologie Intégrative et des Systèmes, Université Laval, Québec-Océan, Québec City, QC, Canada
[c] Institut des sciences de la mer (ISMER), Université du Québec à Rimouski (UQAR), Geotop, Québec-Océan, Rimouski, QC, Canada
[d] The University of Tokyo, Atmosphere and Ocean Research Institute, Kashiwa, Japan
[e] Université de Lille, CNRS, Université du Littoral Côte d'Opale, IRD, UMR 8187, LOG, Laboratoire d'Océanologie et de Géosciences, Station Marine de Wimereux, Lille, France
[f] Département de Biologie, Université Laval, Québec City, QC, Canada

ARTICLE INFO

*Keywords:*
Bioindicators
Ecological monitoring
Anthropogenic impact
Sediment dynamics
Grain-size distribution
Benthic foraminifera
Mineralogical composition
Geochemical tracers
Coastal ecosystems

ABSTRACT

This study investigates the sedimentological, mineralogical, geochemical, and foraminiferal characteristics of three coastal zones in the northwestern Gulf of St. Lawrence: (1) Port-Cartier, (2) the Bay of Sept-Îles (BSI), and (3) Matamec. Sediment samples were analyzed for grain size distribution, mineral and geochemical composition, and benthic foraminiferal assemblages. The results reveal notable spatial variability influenced by local geology, hydrodynamic conditions, and anthropogenic activities. High-energy hydrodynamic conditions at Port-Cartier and Matamec result in predominantly coarse-grained sediments, while variable energy regimes in the BSI produce a heterogeneous mixture of fine and coarse materials. Mineralogical analyses indicate that Port-Cartier and Matamec sediments are rich in quartz, K-feldspar, and amphibole, originating from local granitoid and metamorphic bedrock and are transported northeastward, or westward in case of Matamec by tidal currents. BSI sediments are markedly enriched in iron and organic matter, due to natural geological inputs amplified by anthropogenic activities, particularly in areas influenced by industrial discharge and anticyclonic circulation. Foraminiferal analyses reveal distinct community patterns closely correlated with sedimentological and geochemical variations. Calcareous species, sensitive to elevated metal concentrations, are largely absent in the BSI, where agglutinated foraminifera dominate iron-rich, fine-grained environments. Foraminiferal populations are also sparse or absent near active river deltas and in gravel-rich substrates, reflecting harsh physical conditions, substrate instability, and fluctuating salinity. Ecological indices exp ($H'_{bc}$) and Foram-AMBI further highlight the sensitivity of foraminiferal assemblages to both natural sediment characteristics and subtle anthropogenic stressors. As the first comprehensive foraminiferal study in this region, this research provides essential baseline data and identifies sensitive bioindicators for long-term ecological monitoring, meaningfully advancing our understanding of sedimentary processes and ecological responses to environmental stress in northern coastal ecosystems.

## 1. Introduction

Coastal and estuarine environments are highly dynamic systems that serve as critical ecological and socio-economic hubs (Kennish, 2002). However, they are also vulnerable to various anthropogenic pressures, such as urbanisation (Tanaka et al., 2021), industrialisation (Lee et al., 2024), sewage discharge (Alldred et al., 2024), and rapid climate change. Rising sea levels, warming waters, habitat degradation, and

* Corresponding author. Département de Géographie, Université Laval, Québec-Océan, Québec City, QC, Canada.
*E-mail addresses:* josn0005@uqar.ca, nehajoshi95.ntl@gmail.com (N. Joshi).
[1] Now at Département de biologie, chimie et géographie, Université du Québec à Rimouski, Québec-Océan, Rimouski, QC, Canada.

https://doi.org/10.1016/j.ecss.2026.109828
Received 20 November 2025; Received in revised form 6 February 2026; Accepted 16 March 2026
Available online 17 March 2026

more frequent extreme weather events have intensified stress on these regions (Lotze et al., 2006; He and Silliman, 2019). In this context, sediment analysis is essential for understanding ecosystem dynamics, as sediment composition and distribution reflect both natural processes and human-induced changes. Variations in sediment mineralogy and geochemistry can serve as indicators of environmental shifts, making them valuable tools for monitoring coastal ecosystem health (Desrosiers et al., 2013; Joshi et al., 2025). In addition to these physical and chemical assessments, benthic foraminifera serve as complementary and highly sensitive biological indicators of environmental change in coastal ecosystems (Alve, 1995; O'Brien et al. 2021). These single-celled marine organisms (unicellular eukaryotes) with calcareous (calcite), agglutinated (sedimentary particles bound together by organic cement), or organic tests respond to changes in environmental variables such as salinity (Lee et al., 2015), temperature (Deldicq et al., 2021a; Stuhr et al., 2018), nutrient levels (Humphreys et al., 2018), and pollution (O'Brien et al., 2021).

Beyond their indicative value, benthic foraminifera play a functional role in benthic ecosystems. They can represent up to 50% of the benthic eukaryotic biomass in coastal sediments (Moodley et al., 2000) and contribute significantly to carbon, nitrogen, and phosphorus cycling (Jauffrais et al., 2019; Glock et al., 2025). Their trophic diversity (including bacterivory, herbivory, and carnivory) positions them as key components of benthic food webs (Nomaki et al., 2008; Chronopoulou et al., 2019). In addition, their sediment reworking, bio-irrigation, and influence on bacterial community structure are important to ecosystem functioning (Bouchet and Seuront, 2020; Deldicq et al., 2021b; Langlet et al., 2023). Some species can also store and denitrify nitrate under low-oxygen conditions, contributing up to 70% of benthic nitrogen loss in the North Sea and up to 100% in certain Swedish fjords (Piña-Ochoa et al., 2010; Choquel et al., 2021).

These meiobenthic organisms are ideal for studying both modern and past environments because of their rapid response to environmental changes and excellent preservation in sediment records (Murray, 2006; Jorissen et al., 2018). The relationship between foraminiferal community structure and environmental parameters makes them an invaluable tool for ecological monitoring (e.g., Parent et al., 2021; Nunes et al., 2023) and paleoenvironmental reconstruction (Francescangeli et al., 2016; Sambugaro et al., 2025). Their diversity and community composition provide insights into ecosystem health, especially in regions affected by human activities (Alve, 1995; Armynot du Châtelet et al. 2004). The response of foraminifera to environmental stress is often assessed through abundance (Mojtahid et al., 2006), diversity (Francescangeli et al., 2020), and indicator species (Alve, 2003). Fundamental research on the ecology of benthic foraminifera has led to the development of biotic indices based on species sensitivity and tolerance to pollution (Alve et al., 2009, 2016; Bouchet et al., 2012, 2018, 2021; Barras et al., 2014; Jorissen et al., 2018).

The St. Lawrence system, one of Canada's most densely populated regions and a key aquatic gateway to the Laurentian Great Lakes, faces numerous environmental challenges due to human activities (Plan Saint-Laurent, 2024). The Bay of Sept-Îles (BSI), located in the northwestern Gulf of St. Lawrence, is particularly exposed to industrial activities, such as mineral shipping and port operations, making it a hotspot for potential contamination and ecological stress (Carrière and Le Hénaff, 2018). Despite its vulnerability, few studies have characterized the composition or ecological responses of benthic foraminiferal communities in the BSI (Joshi et al., 2025). While benthic macroinvertebrates have occasionally been monitored in the bay (Dreujou et al., 2020), evidence of disturbed assemblages near industrialized areas of the BSI highlights the need to investigate the more sensitive meiobenthic compartment, which remains largely overlooked.

This paucity of baseline ecological data in the BSI is of concern, given the region's long-standing exposure to anthropogenic stressors. In this context, the three main objectives of this study are: to characterize the sedimentary features of the BSI region and its surrounding areas by analyzing grain size and sediment composition across three different zones: Port-Cartier (Zone 1), the BSI (Zone 2), and Matamec (Zone 3); to evaluate the diversity and community structure of foraminifera within BSI; and to identify potential environmental drivers of changes in the spatial distribution of benthic foraminiferal abundance and community structure.

Overall, this study provides a comprehensive overview of the region's environmental status, identifies key drivers of ecosystem change, and establishes baseline data on benthic foraminiferal communities in the BSI region, addressing a regional knowledge gap and supporting long-term ecological monitoring.

## 2. Regional setting

### 2.1. Geographic context

The study area extends along the northwestern coast of the Gulf of St. Lawrence from Port-Cartier to Matamec (Fig. 1), covering diverse environmental and industrial gradients. Strategically chosen, this transect includes areas with significant industrial activity, such as Port-Cartier and the BSI, as well as a more pristine, less industrialized region around Matamec, allowing for comparative studies of human impacts on the coastal ecosystem.

This region features a mix of saltwater from the Atlantic Ocean and freshwater from the St. Lawrence River, creating a dynamic estuarine environment (Lapointe, 2000; Carrière and Le Hénaff, 2018). Port-Cartier, a major industrial port, primarily serves the mining sector and handles large quantities of iron ore and bulk cargo, leading to localized sediment disturbances from loading and unloading activities (Marine Link, 2024). Tidal patterns in Port-Cartier are semidiurnal, with tidal heights reaching up to 3.4 m, influencing sediment transport and deposition in the area (Government of Canada, 2024). The major rivers flowing into this region are the Sainte-Marguerite River, which drains a watershed of approximately 9524 $km^2$ and whose discharge is regulated by several hydroelectric dams, its average annual discharge is 155 $m^3/s$ (OBV Saguenay, 2015) and the Aux Rochers River, which drains a basin of about 4180 $km^2$ and has an average annual discharge of 111 $m^3/s$ (OBVD, 2019a,b).

The BSI is characterized by estuarine circulation patterns with seaward surface currents and shoreward deep-water currents, influenced by tides, winds, and estuarine dynamics. Currents in the bay are anticyclonic, with surface drifters recording average speeds of 17.4 cm/s and reaching up to 86.6 cm/s (Shaw et al., 2023). The major river discharging into the Bay of Sept-Îles is the des Rapides River, which drains a watershed of approximately 573 $km^2$ and delivers an average annual flow of 16.4 $m^3 s^{-1}$, with flood peaks reaching 38.3 $m^3 s^{-1}$ and low flows around 3.25 $m^3 s^{-1}$. Several smaller rivers, including the Hall, aux Foin, and du Poste rivers, also contribute freshwater and sediment to the system. The Port of Sept-Îles is recognized as an important North American mineral port. Heavy industries, including a large aluminium smelter and iron ore industry raise environmental concerns about sediment contamination from heavy metals due to industrial activities (INREST, 2018; Port of Sept-Îles, 2024). This industrial activity has made the BSI a key site for studying the impacts of human activity on marine ecosystems, with support from environmental monitoring through the Environmental Observatory for the BSI (INREST, 2016).

Matamec, on the other hand, represents a more pristine environment along the transect. Situated in the Matamec Ecological Reserve, this area is minimally impacted by human activity and is dedicated to conservation efforts (Gouvernement du Québec ministère de l'Environnement et de la Lutte contre les changements climatiques, 2022) The semi-diurnal tides and boreal ecosystem of Matamec make it an ideal reference point for understanding natural conditions in comparison to more industrialized areas like Port-Cartier and the BSI. The wild Moisie River drains a watershed of 19,871 $km^2$ and has an annual mean discharge of ~466 $m^3 s^{-1}$, with observed yearly averages ranging from ~502 to

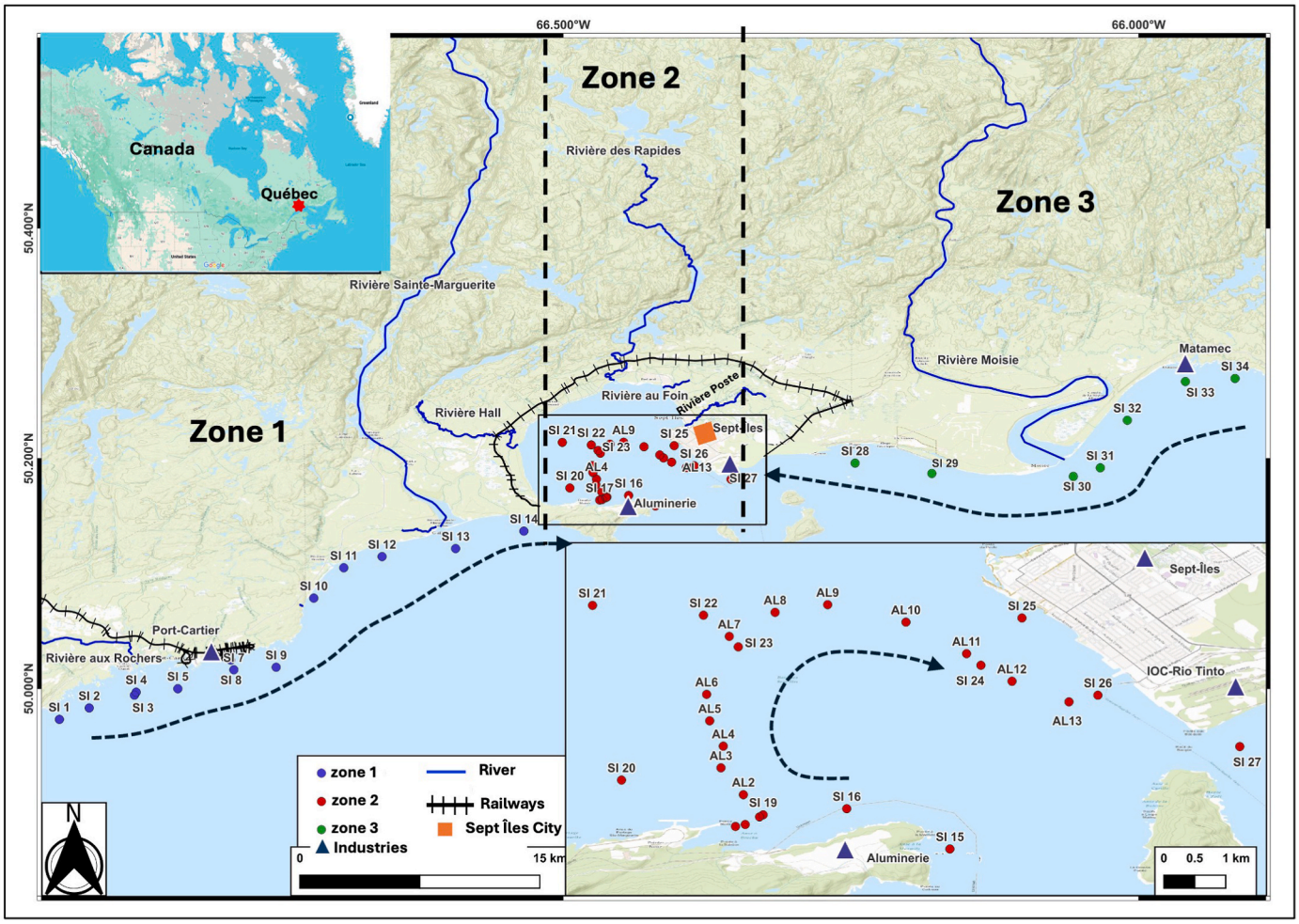


**Fig. 1.** Study site showing all the sampling points and important landmarks. Different colors indicate the different zones. (For interpretation of the references to color in this figure legend, the reader is referred to the Web version of this article).

686 $m^3 s^{-1}$ (Ahmadi-Nedushan et al., 2007). The limited human influence in the region highlights the contrasting environmental pressures and provides a baseline for assessing the extent of human impacts on adjacent, more industrial areas.

### 2.2. Regional geology

The geology of the study area is summarised in Higgins (2005) and Namur et al. (2015). The study area, encompassing Port-Cartier, the BSI, and Matamec on the North Shore of Quebec, is located within the Grenville Province of the Canadian Shield (Fig. 2A). The Grenville Province is composed primarily of high-grade metamorphic rocks formed during the Precambrian era and features a diverse range of igneous and metamorphic rocks, including granitoids, gneisses, and mafic intrusions. In Port-Cartier, the geology is dominated by orthopyroxene-bearing granitoids, charnockites, granodiorites, granites, migmatites, and anorthosites. The region also features gabbros and hypersthene monzonites. However, much of the bedrock in Port-Cartier is covered by littoral deposits, including sand, gravel, and recent fluvial deposits.

Moving eastward, the BSI represents a complex and dynamic coastal environment. The bay encompasses two main physiographic features: a coastal plain and the Sept-Îles Archipelago. The coastal plain is shaped by marine and fluvial terraces that initially formed during the post-glacial Goldthwait Sea transgression during the last deglaciation and were later influenced by the flows of the Sainte-Marguerite and Moisie rivers. These terraces are bordered by the Laurentian Plateau to the north and the Gulf of St. Lawrence to the south. Within the bay, the Sept-Îles Archipelago consists of islands primarily composed of intrusive rocks, part of the Sept-Îles Intrusive Suite (SIIS; Fig. 2B), which dates back to around 540 million years ago. The SIIS is divided into three main units: the Layered Series, the Upper Border Series, and the Upper Series. The Layered Series is mostly composed of gabbro-troctolite, the Upper Border Series contains anorthosite, and the Upper Series includes granite-syenite layers. Fe–Ti oxide layers are notably present in the western part of the intrusion. Extending offshore, these formations intersect with the St. Lawrence Platform, composed mainly of Ordovician limestone. This geological interplay is marked by a post-Ordovician fault system with a southwest-northeast orientation. Over time, coastal erosion has led to the formation of beach terraces and soft cliffs (~30 m) made of postglacial materials. Offshore, sediment thickness varies from 10 to 80 m, with an average sedimentation rate around the archipelago estimated at 0.14 cm/year (e.g., Lajeunesse et al., 2007; Joshi et al., 2025).

Further east, in the Matamec region, the geological composition includes granites, pegmatites, migmatites, and granitoids, accompanied by metasedimentary gneiss and crystalline limestones. Similar to Port-Cartier, the surficial geology of Matamec is characterized by widespread glaciofluvial and fluvial deposits of sand and gravel.

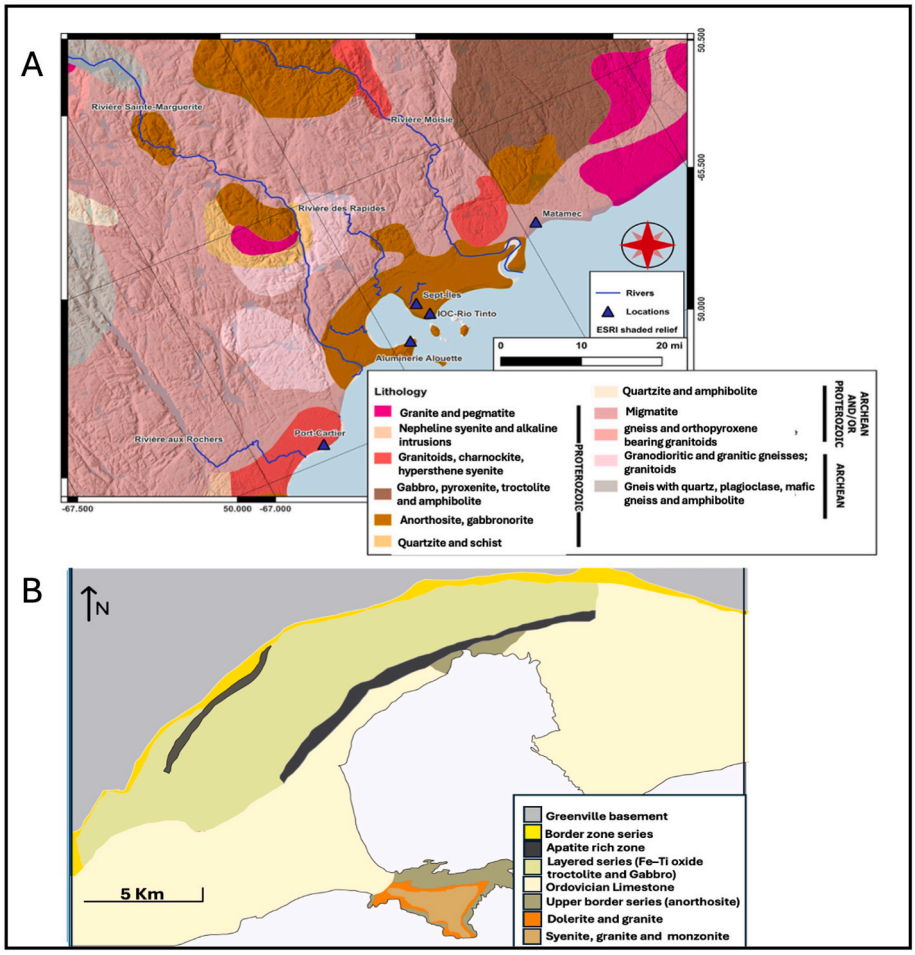


**Fig. 2.** (A) Geological map of the Sept-Îles region (adapted from *Ministère des Ressources Naturelles et des Forêts*, 2002) and (B) Regional geological map of Sept-Îles highlighting the Sept-Îles intrusive suite (modified from Higgins, 2005).

## 3. Methods

### 3.1. Sample collection

A total of 46 surface sediment samples were collected in summer 2021 (June 21-26) and 2022 (June 13-18) using a modified Ponar Grab, specifically designed to prevent sediment mixing and preserve the water-sediment interface. After collection, only the top 1 cm of surface sediments was carefully subsampled from the center of the grab using a 1 cm deep ring and gently scooping with a spatula. One aliquot from each sample was taken for the different analyses. Sediments were stored in the dark at 4 °C in labeled plastic bags until further analysis.

### 3.2. Site grouping and zonation

To capture the spatial variability driven by hydrodynamic conditions and sediment characteristics, sampling sites were divided into three zones along the transect: (1) Port-Cartier, (2) the BSI, and (3) Matamec (Fig. 1). Zone 1 (SI1 to SI15) includes sites located along the coast and at the bay entrance, where stronger circulation, higher energy conditions, and coarser grain sizes dominate due to direct exposure to open marine currents. Zone 2 (SI16 to SI26 and AL1 to AL13) corresponds to the central and inner bay areas, characterized by more restricted water circulation, lower current velocities, and finer-grained sediments. These conditions promote the accumulation of organic matter and metals (Joshi et al., 2025). The reduced hydrodynamic energy facilitates the deposition of fine material and contributes to the observed ecological stress gradients. Zone 3 (SI27 to SI34) represents sites located toward the Matamec sector, where circulation conditions are somewhat more open compared to Zone 2. This zone features intermediate grain sizes and environmental conditions that reflect a transition between sheltered bay environments and more open coastal waters.

### 3.3. Physical and chemical measurements in the water column

Salinity, turbidity, pH, depth, dissolved oxygen and temperature were measured *in situ* during the 2021 field campaign using a Hannah HI 9829 portable multiparameter meter. Water transparency was assessed at each site using a Secchi disk to measure the depth of light penetration. These measurements were conducted systematically at each site to ensure consistent data collection across the study area.

### 3.4. Loss on ignition (LOI) at 550 °C

Loss on ignition was performed at 550 °C to quantify the organic matter content in each sediment sample, following the method outlined in Heiri et al. (2001). Initially, weighed amounts of wet sediment samples were dried in a conventional oven at 105 °C for 24 h. The dried samples were then reweighed and placed in a muffle furnace at 550 °C for 4 h before being weighed again. To ensure no moisture remained, the samples were returned to the conventional oven at 105 °C for 24 h and weighed one final time.

### 3.5. Grain-size analysis

Sediment grain size analyses (<2 mm fraction) were conducted using a Horiba (model LA950v2) laser diffraction grain size analyzer. Before the analyses, approximately 0.2 g of ignited sediment samples were moistened with distilled $H_2O$ and deflocculated by adding 30 mL of a Calgon solution (sodium hexametaphosphate; 20 g $L^{-1}$) and disaggregated using an in-house rotator for 12 h prior to measurement. The grain size distribution (clay, silt, sand) and statistical parameters (e.g., $D_{50}$) were calculated using GRADISTAT software version 9.1 (Blott and Pye, 2001).

### 3.6. Energy dispersive X-ray fluorescence analyses

Eleven elements (Al, Si, K, Ca, Ti, Mn, Fe, V, Sr, Zr) were analyzed using energy dispersive X-ray fluorescence (EDXRF) spectrometry with the Malvern Panalytical Epsilon 3-XL instrument, following the procedure described by Gamboa et al. (2017). The selection of elements was based on the main anthropogenic activities in the Bay of Sept-Îles, which include mineral shipping and port operations, a large aluminium smelter, and iron ore mining. Accordingly, elements such as Fe and Mn, together with associated trace metals (e.g., Ti, Zn and V), were selected as potential tracers of industrial inputs, as their enrichment has been documented in bay sediments during the post-industrial period (Joshi et al., 2025). Before ED-XRF analysis, loss on ignition was determined gravimetrically by heating the dried samples to 950 °C for 3 h. Approximately 0.6 g of the ignited samples was then treated by borate fusion (pure composition of 49.75% $Li_2B_4O_7$, 49.75% $LiBO_2$, and 0.5% LiBr) in an automated fusion furnace (CLAISSE® M4 Fluxer) to create glass disks. Following the preparation, the samples were analyzed, and the resulting ED-XRF spectra were processed using the standardless Omnian software package (Malvern PANalytical). The results were reported as weight percentage (wt.%) for major elements (Al, Si, K, Ca, Ti, Mn, Fe) and micrograms per gram (μg/g) for trace elements (V, Zn, Sr, Zr). Procedural blanks, prepared with synthesized silicon oxide powder (99.999% $SiO_2$; American Elements; SI-OX-05M-P.325 M), consistently represented less than 1% of the lowest concentration measured in the sediment samples. The precision and accuracy of the analysis were validated against international standards (USGS SDC-1 and BCR-2) and through replicate sample analysis. Deviations were found to be within the range of 1–8% for major elements and 5–11% for trace elements, ensuring high analytical reliability.

### 3.7. Quantitative X-ray diffraction (qXRD)

For qXRD analysis, around 1 g of each sediment sample was mixed with 0.25 g of corundum, serving as an internal standard. The samples were finely ground in a McCrone micronizing mill using 5 mL of ethanol to create a uniform powder. The resulting slurry was dried overnight in an oven at approximately 60 °C and subsequently homogenized using an agate mortar. To avoid agglomeration of fine particles, 0.5 mL of Vertrel was added. The dried and homogenized powder was sieved to less than 300 μm, loaded into sample holders, and analyzed with a Malvern Panalytical X'Pert Powder diffractometer.

XRD scans were conducted over a range of 5° to 65° 2θ with a step size of 0.02° 2θ and a counting time of 4 s per step. The resulting diffraction data were converted into mineral weight percent (wt.%) using the R package "*powdR*" (Butler and Hillier, 2021). *powdR* uses a full pattern summation approach that permits the quantification of whole-sediment mineralogy with an average absolute bias of 0.6% for non-clay minerals, 2% for clay minerals, and 5% for amorphous phases (Butler and Hillier, 2021). The total mineral content was normalized to 100%. The analysis quantified 15 key minerals: quartz, K-feldspar, plagioclase, calcite, dolomite, amphibole, Fe-bearing minerals, amorphous silica, kaolinite, chlorite, illite, biotite, muscovite, smectite, and vermiculite. These minerals accounted for more than 96% of the total mineral content in the bulk sediment samples.

### 3.8. Foraminifera analysis

The foraminiferal analysis was conducted on 46 surface sediment samples, following the protocols outlined by de Vernal et al. (1999). For each sample, 10 $cm^3$ of wet sediment was measured, dried at ambient temperature, and re-weighed. The dried samples were then wet-sieved and collected between 63 and 500 μm mesh sieves, and the resulting fractions were examined under a binocular microscope at magnifications of 40× and 80x. Agglutinated and calcareous benthic foraminifera were hand-sorted using a paintbrush. Living and dead specimens were pooled and treated as a single total assemblage for all subsequent analyses. Identification and enumeration followed the taxonomic classifications of Rodrigues (1980), Loeblich and Tappan (1987), and The World Foraminifera Database (Hayward et al., 2024). Sites with fewer than 10 total individuals were classified as barren and excluded from numerical analyses.

Abnormalities were classified following the general approach of Polovodova and Schönfeld (2008). Test abnormalities were identified visually based on external morphology, without the use of staining procedures.

### 3.9. Foraminiferal ecological quality status (EcoQS)

To assess the ecological quality of benthic environments, we calculated the exponential of the Shannon diversity index, exp ($H'_{bc}$), for living foraminiferal assemblages at each site. Species abundances were compiled for the >63 μm fraction in surface (1 cm) sediment layer, and Shannon diversity ($H'_{bc}$) was computed using the natural logarithm. The exponential transformation, exp ($H'_{bc}$), was applied to account for both species richness and evenness, and to approximate the effective number of abundant species. Following the classification proposed by Bouchet et al. (2012) for living foraminifera, sites were assigned an Ecological Quality Status (EcoQS) based on exp ($H'_{bc}$) thresholds:

- exp ($H'_{bc}$) > 15: High
- 10 < exp ($H'_{bc}$) ≤ 15: Good
- 5 < exp ($H'_{bc}$) ≤ 10: Moderate
- exp ($H'_{bc}$) ≤ 5: Poor

### 3.10. Foram-AMBI calculation

Foram-AMBI (Foraminiferal AZTI Marine Biotic Index) is a tool used to assess environmental quality based on the composition of benthic foraminiferal communities. Since diversity metrics alone may not fully capture the impacts of environmental stressors, especially where tolerant species dominate low-diversity communities, species-based indices such as Foram-AMBI is used to better characterize environmental conditions. This methodology involves assigning each species within the community to one of five ecological groups (EGs), ranging from sensitive species that thrive in undisturbed environments (EG I) to highly opportunistic species that tolerate or thrive in heavily impacted or polluted areas (Alve et al., 2016; Jorissen et al., 2018).

The ecological groups (EGs) are defined as follows:

- EG I (Sensitive species): Species abundant in pristine, low-organic conditions.
- EG II (Indifferent species): Species present across a range of organic matter levels but absent in highly polluted areas.
- EG III (Third-order opportunists): Species tolerant of low to moderate organic enrichment.
- EG IV (Second-order opportunists): Species showing a positive response to organic enrichment.
- EG V (First-order opportunists): Highly opportunistic species that dominate in heavily impacted conditions.

In the present study, the list from Alve et al. (2016) was used as it was developed in similar latitudes and habitats. Once species were assigned to these ecological groups, the Foram-AMBI index was calculated using the following formula:

$$\text{Foram} - \text{AMBI} = \{(0 \times \%\text{EG I}) + (1.5 \times \%\text{EG II}) + (3 \times \%\text{EG III}) + (4.5 \times \%\text{EG IV}) + (6 \times \%\text{EG V})\} / 100$$

In this formula, %EG I to %EG V represent the relative abundance (in percentages) of species in each ecological group within a sample. The Foram-AMBI score is then interpreted based on its value, where lower values indicate a less impacted environment, while higher values signify greater environmental stress or degradation. This methodology allows for a quantitative assessment of environmental quality in marine ecosystems based on the community structure of foraminifera.

As indicated by Parent et al. (2021), the range for the interpretation of the Foram-AMBI index is as follows:

- $0 < \text{AMBI} \leq 1.4$: High status or "unpolluted"
- $1.4 < \text{AMBI} \leq 2.4$: Good status or "slightly polluted"
- $2.4 < \text{AMBI} \leq 3.4$: Moderate status or "polluted"
- $3.4 < \text{AMBI} \leq 4.4$: Poor status or "transition to heavily polluted"
- $4.4 < \text{AMBI} \leq 6$: Bad status or "heavily polluted"

### 3.11. Statistical analysis

Multivariate analysis was conducted using R (R Core Team, 2024) to assess patterns in sediment mineralogy and geochemistry. Raw data were imported from Excel using the readxl package (Wickham and Bryan, 2023), and sample identifiers were extracted for use as row labels. Site zones were defined manually based on sampling location and encoded as categorical variables using the case_when() function (*dplyr* package; Wickham and Bryan, 2023).

All variables were converted to numeric format, and columns with >50% missing values were removed. A Spearman correlation (r) was computed to identify multicollinearity and variables with high pairwise correlations ($r > 0.7$) were excluded based on geochemical redundancy. The filtered dataset was scaled using the scale () function to standardize units across variables.

**Principal Component Analysis (PCA)**: PCA was performed using the PCA() function from the *FactoMineR* package (Lê et al., 2008), and visualizations were produced using *factoextra* (Kassambara & Mundt, 2016 ). These included a scree plot of eigenvalues, variable contribution plots, PCA ordination of sites colored by zone, and a biplot combining site scores and variable loadings. Variables contributing most strongly to each principal component were identified from the loadings matrix and used to interpret dominant environmental gradients. Differences in sedimentological and mineralogical variables among Zones were tested using the Kruskal–Wallis test. Statistical significance was evaluated at p-values $<0.05$.

**Species diversity and composition analysis:** Diversity analyses were conducted in R (R Core Team, 2024). Species data, imported using *readxl*, were used to compute Shannon and Simpson indices with the *vegan* package (Oksanen et al., 2020). Results were saved using *openxlsx* (Schauberger and Walker, 2014) Species distributions across species were visualized using stacked bar plots created with *ggplot2* (Wickham, 2023), reshaped using *reshape2* (Wickham, 2024), and enhanced with a custom color palette.

**Redundancy analysis:** Redundancy Analysis (RDA) was used to evaluate relationships between species abundance and environmental variables (grain size, ED-XRF, qXRD). Datasets were processed using *readxl*, *vegan*, and *ggplot2*. Species data were Hellinger-transformed using decostand (), and environmental data were log-transformed (log (x+1)) to correct for skewness. RDA results were visualized as biplots showing gradients (arrows), species (initials), and site positions. The significance of the RDA model and explanatory variables was assessed using Monte Carlo permutation tests (999 permutations).

Finally, spatial distribution maps were created in QGIS (version 3.34; QGIS Development Team, 2024).

## 4. Results

### 4.1. Grain size

The grain size analysis of the sediment samples collected across the three zones revealed distinct patterns in the distribution of gravel, sand, silt, clay, and particle size ($D_{90}$) within each Zone (Fig. 3; Table 1).

Zone 1 exhibited an average sediment composition of 2% gravel, 92% sand, and 6% silt, with no detectable clay content. The average $D_{90}$ value for this Zone was 1135 μm, indicating the dominance of sand-sized particles. Gravel content occasionally exceeded the Zone average, reaching a maximum of 23%, while silt content peaked at 29%, significantly higher than the average. Clay was absent throughout the zone, and the maximum $D_{90}$ value recorded was 4877 μm, reflecting the presence of coarser sediment particles.

Zone 2 had an average sediment composition of 46% sand, 52% silt, and 2% clay, with no gravel detected. The average $D_{90}$ value for the Zone was 402 μm, indicating a finer sediment profile compared to Zone 1. Sand content peaked at 99%, while the highest silt concentration reached 84%, both significantly above the Zone average. Clay content was minimal, with a maximum of 8.4% observed, and the coarsest sediment particle size was reflected by the maximum $D_{90}$ value of 669 μm.

Zone 3 had an average sediment composition of 4% gravel, 60% sand, and 37% silt, with no clay detected. The average $D_{90}$ value for this Zone was 810 μm, indicating the presence of relatively coarse-grained particles, though not as large as those found in Zone 1. Gravel content peaked at 22%, making it the most gravel-rich area in the zone. Sand content reached a maximum of 90%, indicating a predominantly sandy site. The highest silt content, at 69%, was significantly above the Zone average, highlighting the variability within the zone. The coarsest sediment particles were reflected by a maximum $D_{90}$ value of 2946 μm.

### 4.2. Physical and chemical properties of the water column

The sites exhibited relatively stable pH values, ranging from 8 to 8.9 (Fig. 4), with a mean of 8.5. Surface temperatures varied between 10.6 °C and 14.7 °C, averaging 12.4 °C. Zone 2 showed slightly higher temperatures (13.1 °C) compared to Zone 1 (11.7 °C), river sites (12.6 °C), and Zone 3 (12 °C) (Fig. 4). The sampling sites had a mean depth of 20 m, ranging from 4 to 54 m, with the deepest sites located in Zone 3. Dissolved oxygen concentrations ranged from 6.9 mg/L to 8.6 mg/L, with a mean value of 7.4 mg/L and a median of 7.3 mg/L across sites. Turbidity ranged from 0 to 2 FNU, with an average of 0.4 FNU, remaining near-zero in Zones 1 and 3, and slightly higher in Zone 2. Salinity varied between 19.6 PSU near river estuaries and 30.5 PSU, averaging 28.6 PSU across all sites. Salinity remained generally stable across most of the study area, with localized fluctuations near the mouths of the Sainte-Marguerite River (SI13) and the Moisie River (SI30–31). In Zone 2, salinity was particularly consistent, ranging narrowly between 29.2 and 29.8 PSU.

### 4.3. Quantitative X-ray diffraction (qXRD)

Mineral composition varied across the three zones (Fig. 5), reflecting distinct sediment sources. Plagioclase was the dominant mineral in all three zones, with median values of ~37% in Zones 1-2 and ~40% in Zone 3, the latter being significantly higher ($p < 0.05$). Quartz contributed notably in Zones 1 (~23%) and 3 (~19%), both significantly higher than in Zone 2 ($p < 0.05$). K-feldspar was more abundant in Zones 1-2 (~16-18%) compared to Zone 3 (~13%). Zone 1 was distinguished by significantly higher variability in clay mineral contents (ranging from

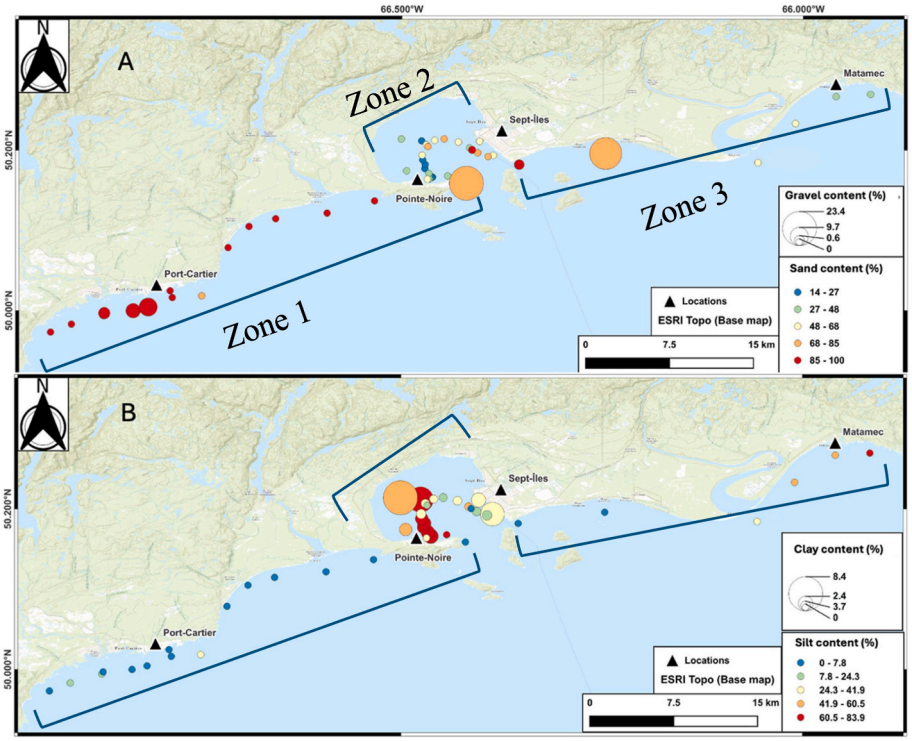


**Fig. 3.** Variation in sediment grain-size composition along the Port-Cartier to Matamec transect: (A) Sand and gravel and (B) Silt and clay content.

**Table 1**
Average grain size composition and particle size ($D_{90}$) along the transect from the three zones studied here.

| Zone | Gravel (%) | Sand (%) | Silt (%) | Clay (%) | $D_{90}$ (μm) |
|---|---|---|---|---|---|
| **1** | 2 | 92 | 6 | 0 | 1135 |
| **2** | 0 | 49 | 48 | 2 | 402 |
| **3** | 4 | 60 | 37 | 0 | 810 |

0 to >15%) compared to Zones 2 and 3 ($p < 0.05$). Zone 2, while comparable to Zone 1 in plagioclase abundance, was characterized by significantly higher concentrations of apatite (~1.7%) and Fe-oxides (~4-5%) than either Zone 1 or Zone 3. Zone 3 showed more homogeneous distributions of major minerals, with narrower interquartile ranges in quartz and plagioclase relative to Zone 1. Pyroxene occurred at low levels (1–4%) in all zones, with slightly lower values in Zone 3 ($p < 0.05$). Amphibole (~11-12%) and dolomite (<2%) showed no significant differences among zones. Among all minerals, quartz ($p = 0.0076$), K-feldspar ($p = 0.0257$), and Fe-oxides ($p < 0.0001$) showed statistically significant differences between zones, with Fe-oxides emerging as the most discriminating component.

### 4.4. *Energy dispersive X-ray fluorescence analyses*

To evaluate whether the observed inter-zone differences were statistically significant, each element was tested using the Kruskal-Wallis test. Among all elements, only aluminum ($p = 0.0388$) and silicon ($p = 0.0539$) showed statistically significant or near-significant differences across zones. Although most other elements did not reach statistical significance, their spatial trends remain relevant in interpreting sediment provenance and depositional variability and are presented here for completeness.

Si was the dominant element across all zones, with slightly lower values in Zone 2 (29 %) compared to Zones 1 and 3 (30 %) Fig. 6. Al and

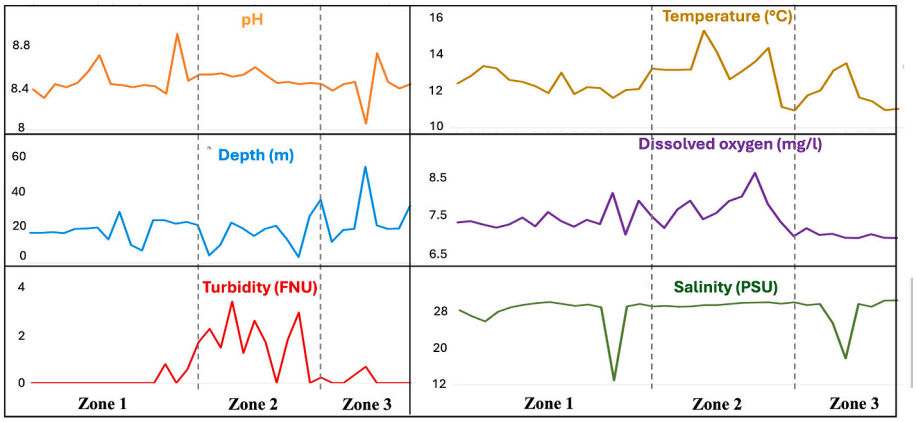


**Fig. 4.** Environmental parameters along the study site: pH, temperature, depth, dissolved oxygen, turbidity, and salinity. Sites are ordered west to east, from left to right.

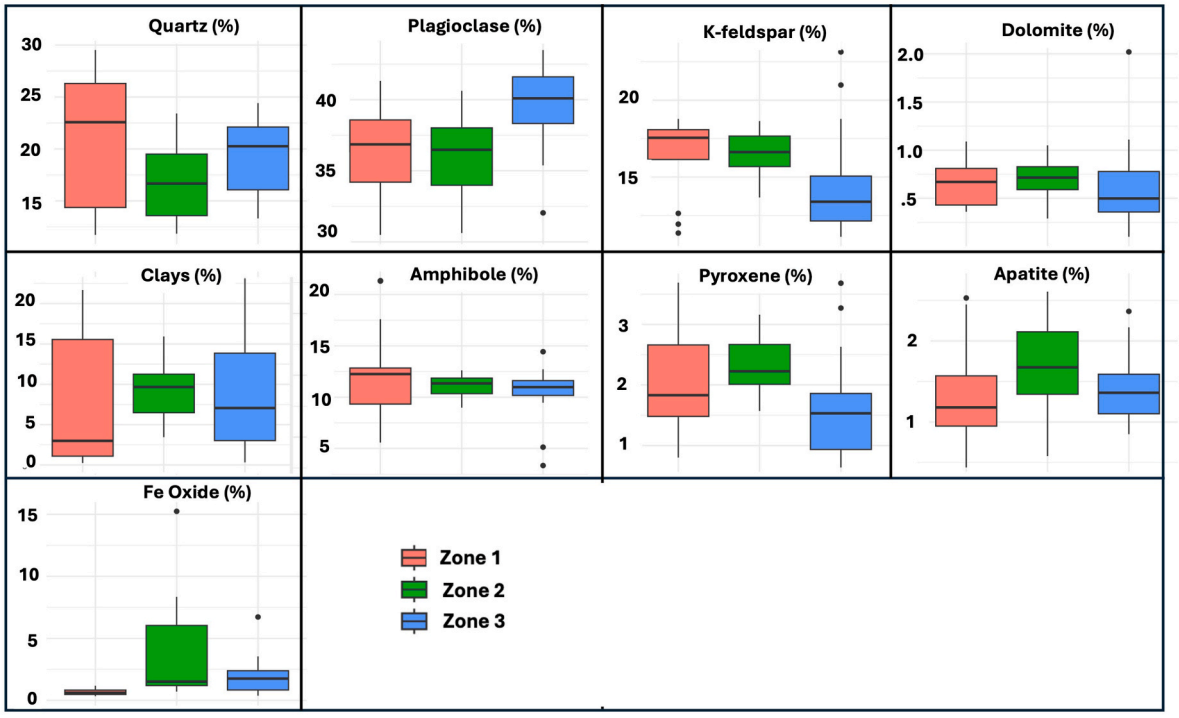


**Fig. 5.** Box plot showing mineralogical variability along the three zones.

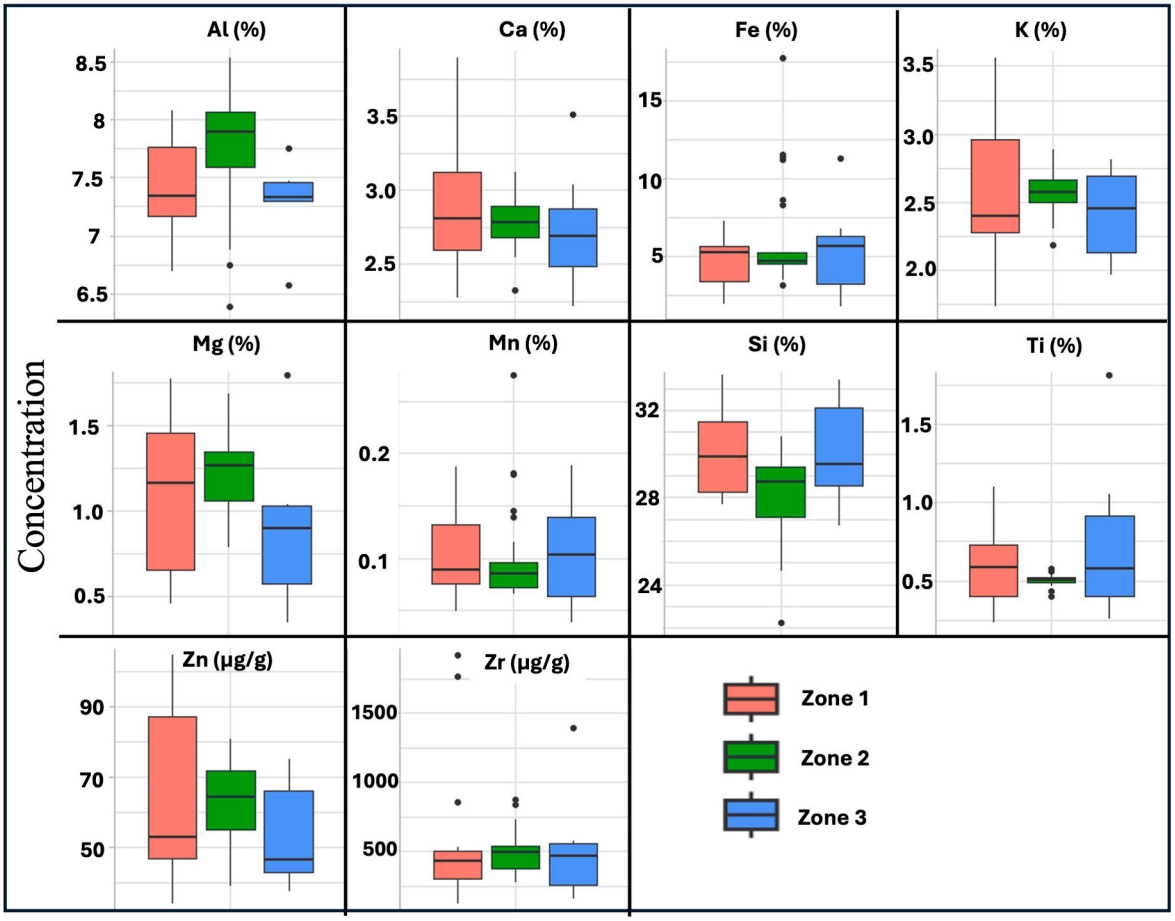


**Fig. 6.** Box plot showing geochemical variability along the three zones

Ca remained stable (7-8 % and ~2.7-2.8 %, respectively), while K and Mg were modestly enriched in Zone 2. Fe showed the strongest contrast, with higher values in Zone 3 (6.0 %) relative to Zones 1 (5.3 %) and 2 (4.7 %). Among trace elements, Ti and Mn were consistently low, whereas Zn was most abundant and variable in Zone 1 (34-105 μg/g), and Zr was slightly enriched in Zone 2. Extreme outliers characterized Fe and Mn in Zone 2 and Zr in Zone 1, indicating localized enrichment. Overall, Zone 2 was distinguished by elevated Mg, K, Zn, and extreme Fe–Mn variability, while Zone 1 showed greater compositional heterogeneity and Zn enrichment.

### 4.5. Principal component analysis

The PCA biplot based on qXRD and ED-XRF data explained 49% of the total variance (Fig. 7). The most influential variables were Fe, Mn and organic matter as indicated by their long red arrow vectors, reflecting high contributions. In contrast, K-feldspar, clay and dolomite showed minimal influence, represented by short arrows with low contribution values (blue to violet gradient). The biplot highlighted a distinct clustering of Zone 2 sites, suggesting a unique mineralogical and geochemical configuration compared to Zones 1 and 3. This distinction is visually evident though their consistent alignment with metal associated vectors in the first two quadrants. Sites from Zone 1 are mainly distributed in quadrants III and IV and are positioned closer to vectors representing quartz, plagioclase, and zircon. However, SI1, SI2, SI4, and SI7 plot nearer to the vectors associated with Zn and silt. Sites from Zone 2 are primarily clustered in quadrants I and II. In particular, SI16–SI20 plot closer to Fe and FeOx, while the AL sites are located nearer to vectors representing Sr, Al, Ti, OM, and silt. Zone 3 sites are mainly distributed across quadrants III and IV, with several sites positioned closer to vectors representing plagioclase, pyroxene, and K.

### 4.6. Organic matter distribution

Fig. 8 illustrates the distribution of organic matter (OM) and Fe content across the study sites. In Zone 1, OM content ranged from 0.5% to 5.1%, with the site SI9 showing the highest value. In contrast, sites SI11 and SI12 had the lowest values at 0.4% and 0.5%, respectively. In Zone 2, OM content was higher than in the other zones. Sites SI21 and SI20 had values of 5.1% and 4.3%, respectively, while SI16 recorded 4.0%. The AL sites within this Zone showed consistently high OM content, with AL4 and AL5 at 5.1% and 4.9%, respectively, while AL6 had a relatively lower value of 1.9%. In Zone 3, OM content was the lowest, ranging from 0.8% to 1.4%, with site SI30 showing the highest value.

### 4.7. Foraminiferal analysis

#### 4.7.1. Foraminiferal spatial distribution patterns

Foraminiferal counts did not consistently meet the standard minimum of 300 individuals, with notably low counts in Zones 1 and 3, while Zone 2 showed higher counts, reaching up to 350 individuals. Despite these variations, the distribution of foraminifera along the transect revealed distinct patterns of species dominance and diversity, reflecting the unique environmental conditions across the different zones. Two groups of deformities were observed in Zone 2: chamber abnormalities and test abnormalities. Chamber abnormalities included deviations affecting the

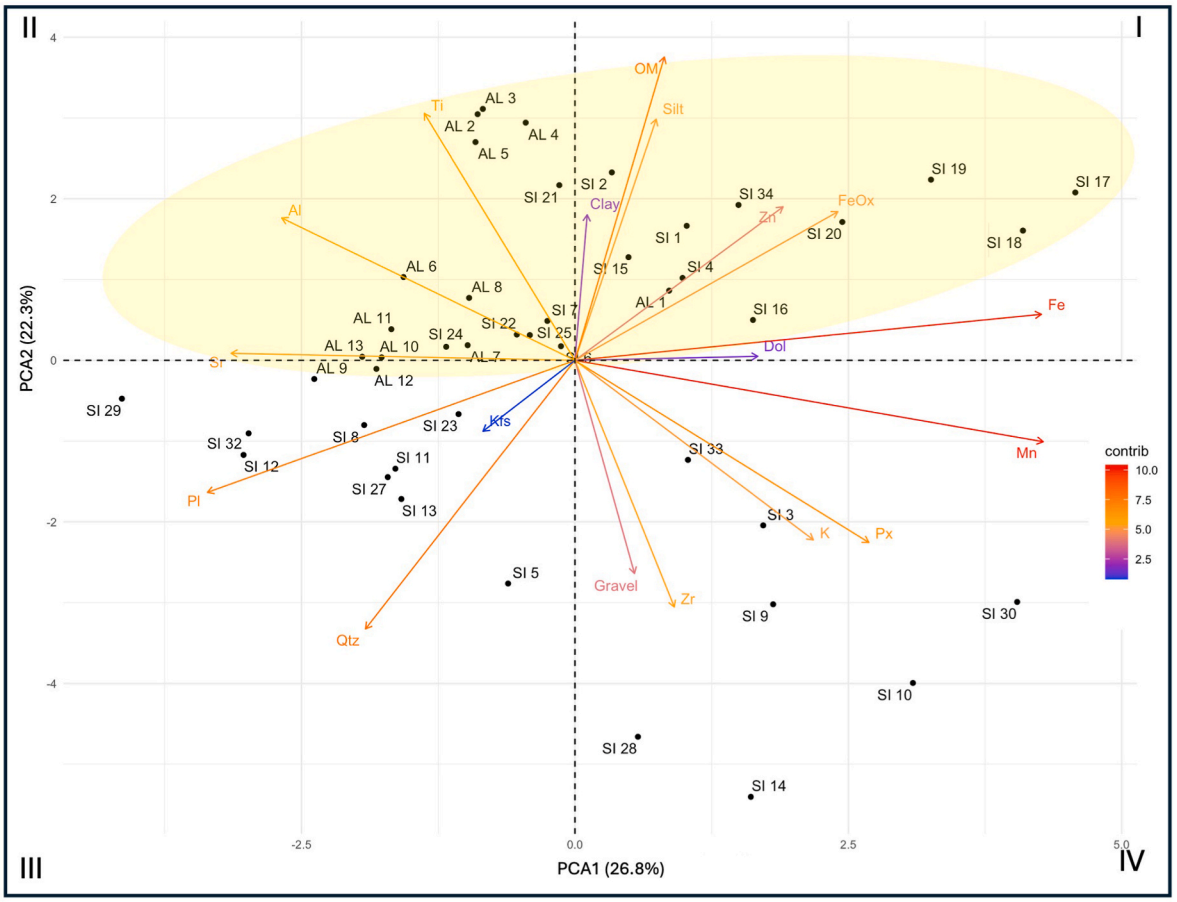


**Fig. 7.** PCA biplot visualizing site distribution and mineral–geochemical associations across different zones, based on qXRD and ED-XRF data. Variable contributions are shown as arrows, colored by their influence on the PCA axes. The yellow oval highlights a cluster of **Zone 2 sites** sharing similar geochemical and mineralogical characteristics. (For interpretation of the references to color in this figure legend, the reader is referred to the Web version of this article.)

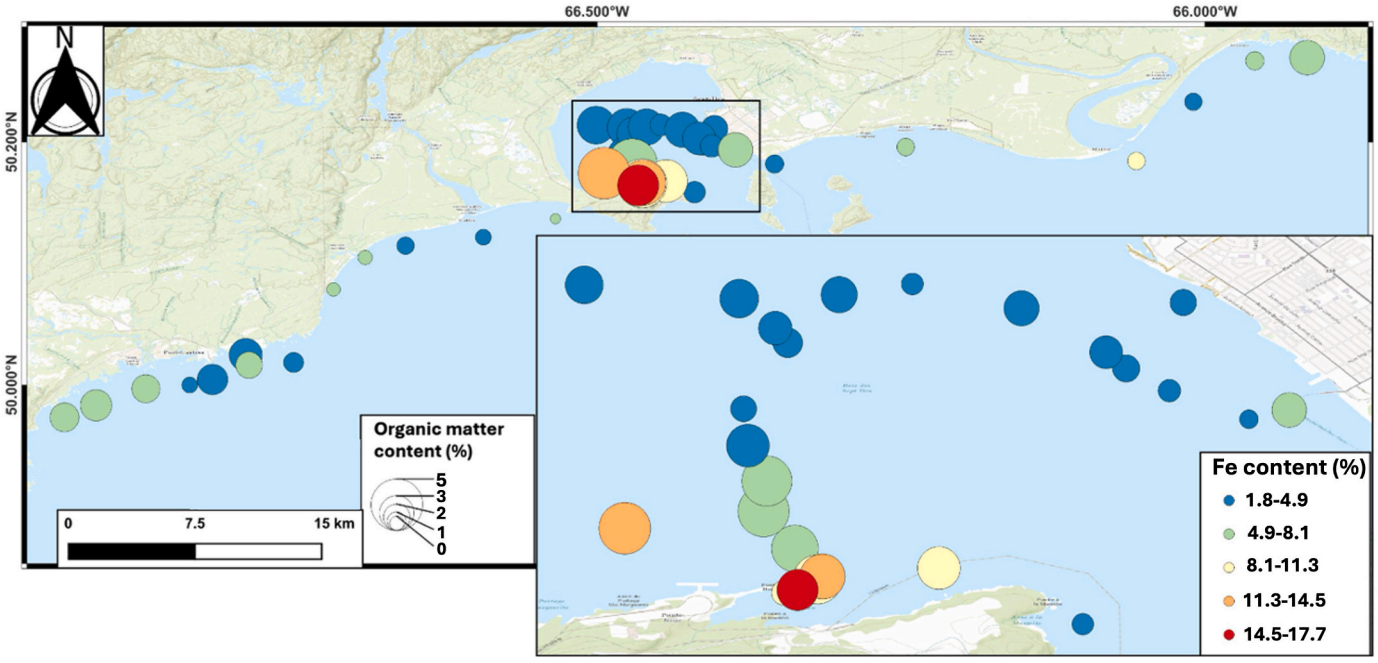


**Fig. 8.** Spatial distribution of iron and organic matter along the three zones.

individual chambers, such as aberrant chamber shape or protruding chambers. Test abnormalities referred to deformations affecting the overall shell structure, including twisted forms, compressed tests, twinning (fusion of two individuals), and general distortion.

**Zone 1:** In this zone, several sites were barren (SI3, SI4, SI6, SI11, SI13, SI14, and SI15). Among the sites where forams were found, the highest total abundance was recorded at SI9 (212 individuals), while the lowest was observed at SI12 (20 individuals). Among calcareous taxa, *Cibicidoides wuellerstorfi* was the most dominant species at SI9, contributing 30%, while it reached 15% at SI10. *Cornuspira planorbis* contributed 7% at SI10. *Islandiella norcrossi* was dominant at SI12, where it accounted for 30% of the assemblage. In contrast, agglutinated species were generally sparsely present in this zone. Among them, *Eggerella advena* showed notable occurrences, contributing 31% at SI1, 19% at SI2, and reached its highest proportion of 47% at SI7. Additional agglutinated forms such as *Textularia earlandi*, *Spiroplectammina biformis*, and *Cribrostomoides* sp. were sporadically present but in lower abundances. The absence of foraminifera at several sites was consistent with sedimentological observations, where elevated gravel content and coarse sediment fractions likely limited foraminiferal colonization. No deformities were observed in this zone.

**Zone 2:** This Zone exhibited the lowest species richness but the

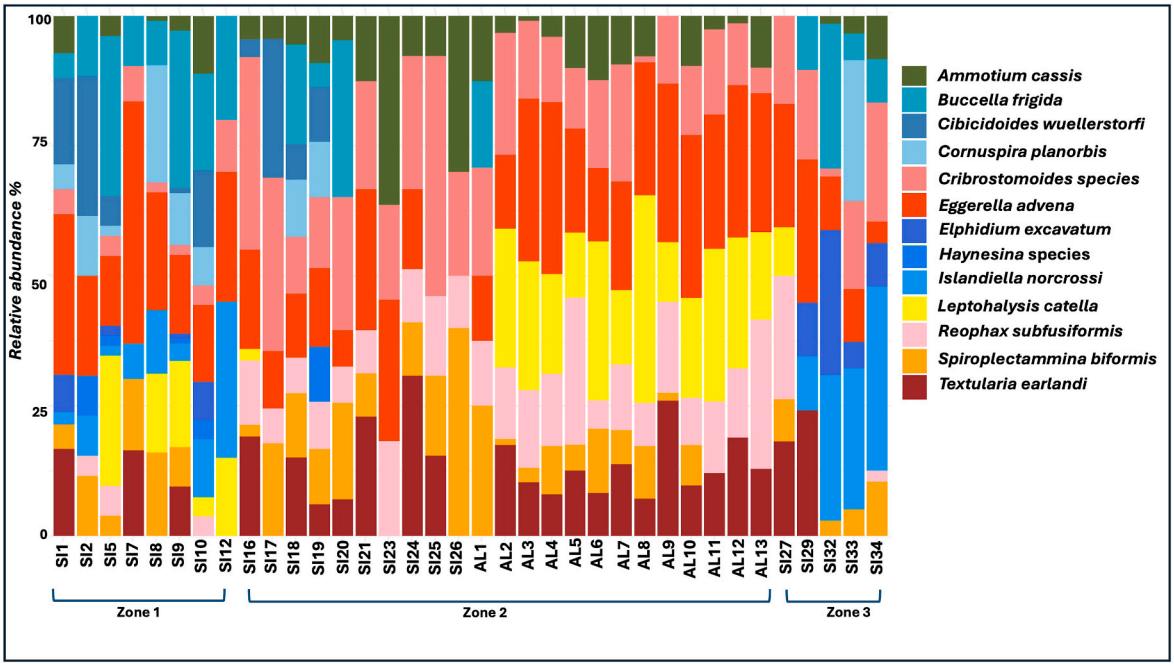


**Fig. 9.** Stacked bar plot showing the abundance and distribution of foraminifera across the study zones (calcareous species are in shades of blue and agglutinated species are in warm colors). (For interpretation of the references to color in this figure legend, the reader is referred to the Web version of this article.)

highest overall abundance of foraminifera, with a strong dominance of agglutinated species (Fig. 9). Total abundances ranged from 45 individuals at SI17 to 363 individuals at AL1. Lower abundances were observed at the eastern bay sites, while western sites exhibited higher concentrations. Sites SI23, SI25, and SI26 were barren.

*Leptohalysis catella* was the most dominant taxon across the sites, with relative abundances ranging from 15% to 40%, reaching maximum dominance at AL5 and AL7. *Eggerella advena* was the second most abundant species, reaching 33% at SI21, 31% at AL11, and 31% at AL9. Other agglutinated species, including *Reophax subfusiformis* (24.77% at AL2, 23.75% at AL13) and *Ammotium cassis* (up to 12.33% at AL5), were also frequently recorded.

In contrast, calcareous species were rare in this zone, contributing only 2% to the total assemblage. *Cibicidoides wuellerstorfi*, *Buccella frigida*, and *Elphidium excavatum* were observed in very low numbers at nearshore sites (SI18 to SI22) but were entirely absent from the AL stations.

Deformed specimens were recorded at SI18, SI19, and AL1, representing ~4%, 18% and 17% of the total assemblages, respectively. The observed deformities included shell protrusions in *Cibicidoides wuellerstorfi* and *Elphidium excavatum*, twinning anomalies and twisted tails in *Eggerella advena* and *Spiroplectammina biformis* (Fig. 10). Deformed specimens were observed exclusively at sites SI18, SI19, and AL1, where iron concentrations were among the highest recorded (Fe = 13-18%; Fig. 8).

**Zone 3:** This Zone exhibited a marked reduction in both diversity and species abundance, with sites SI28, SI30, and SI31 being entirely barren. *Textularia earlandi* was notably abundant at Site SI29, comprising 28% of the species present. In contrast, *Islandiella norcrossi* dominated sites SI32, SI33, and SI34, with relative abundances of 28%, 27%, and 35%, respectively. Other species observed in this Zone included *Cribrostomoides* sp (22%)., *Spiroplectammina biformis* (10%) and *Eggerella advena* (4%).

In Zone 1, agglutinated and calcareous species were nearly equally represented, comprising 49% and 51% of the assemblage, respectively. A striking contrast was observed in Zone 2, where agglutinated species overwhelmingly dominated, at 98%, leaving calcareous species at only 2%. In Zone 3, the assemblage again showed a more balanced distribution, with agglutinated species accounting for 57% and calcareous species for 43% (Fig. 11).

#### 4.7.2. Foraminiferal diversity and corresponding ecological quality status

Zone 1 exhibited the highest ecological quality and community diversity among all three zones. The exp ($H'_{bc}$) values ranged from ~5 at Site SI7 and SI12 (Poor) to 9.3 at Site SI9 (Moderate), with the majority of sites showing Moderate EcoQS (Fig. 12). Species richness in this zone was relatively high, ranging from 5 species (SI12) to 12 species (SI9), the highest recorded in the entire study. These findings suggest that Zone 1 supports well-structured, stable benthic foraminiferal communities with greater evenness and richness.

Zone 2 presented a wider range of ecological quality, with exp ($H'_{bc}$) values between 3.5 (SI26) and 8.5 (SI18). Most sites fell under the Moderate EcoQS category, although several sites (e.g., SI23, SI25, SI26) were classified as Poor. Species richness varied from 4 species (SI23, SI26) to 9 species (SI18), showing a mosaic of environmental conditions. This heterogeneity could reflect localized stressors or transitional conditions affecting specific sites within the zone.

Zone 3 displayed the lowest values of both diversity and ecological quality. The exp ($H'_{bc}$) ranged from 3.5 at SI29 (Poor) to 5 at SI33 and SI34 (Moderate), with most sites classified as Poor in terms of EcoQS. Species richness was also limited, typically ranging from 4 to 7 species. This reduced taxonomic richness likely contributes to the lower EcoQS scores observed in this zone, highlighting that species richness can significantly influence ecological quality assessments based on diversity indices.

#### 4.7.3. Foram-AMBI index

Fig. 13 presents the Foram-AMBI index values for each site, along with their corresponding environmental quality status, ranging from unpolluted to heavily polluted conditions. In Zone 1 (SI1 to SI15), most sites displayed conditions ranging from good to poor, with AMBI values varying from 2 (SI9) to 4 (SI8). Notably, SI1, SI7, and SI8 exhibited

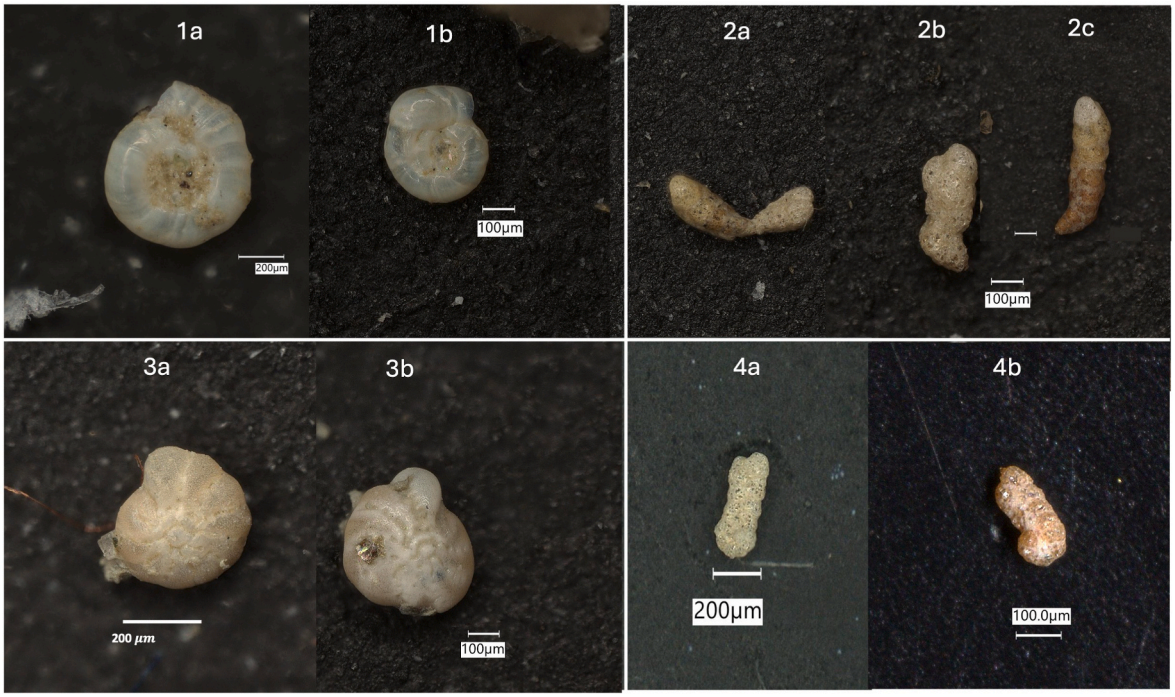


**Fig. 10.** Morphological deformities observed in benthic foraminifera from the bay. Specimens labeled **a** represent normal forms, whereas panels b–c illustrate deformed morphologies. (1b) *Cornuspira planorbis* showing distorted coiling; (2b, c) *Eggerella advena* displaying malformed test growth (siamese-twin, twisted, and crooked forms); (3b) *Elphidium excavatum* exhibiting protruded shell development; (4b) *Spiroplectammina biformis* showing irregular test elongation.

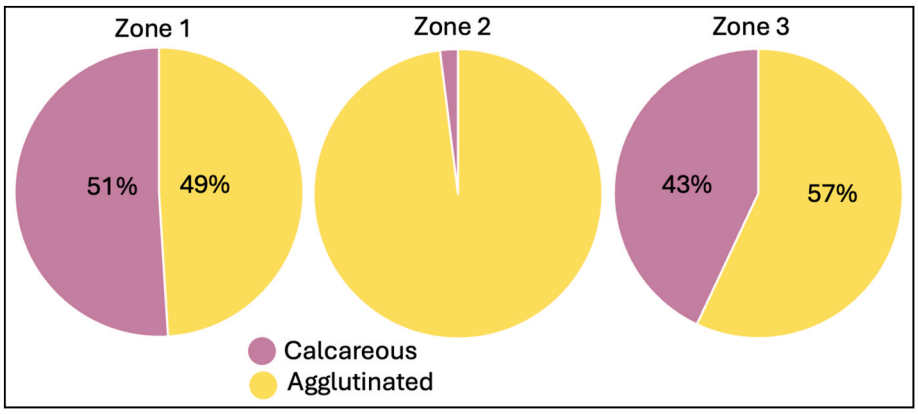


**Fig. 11.** Proportional distribution of agglutinated and calcareous foraminifera along the three zones.

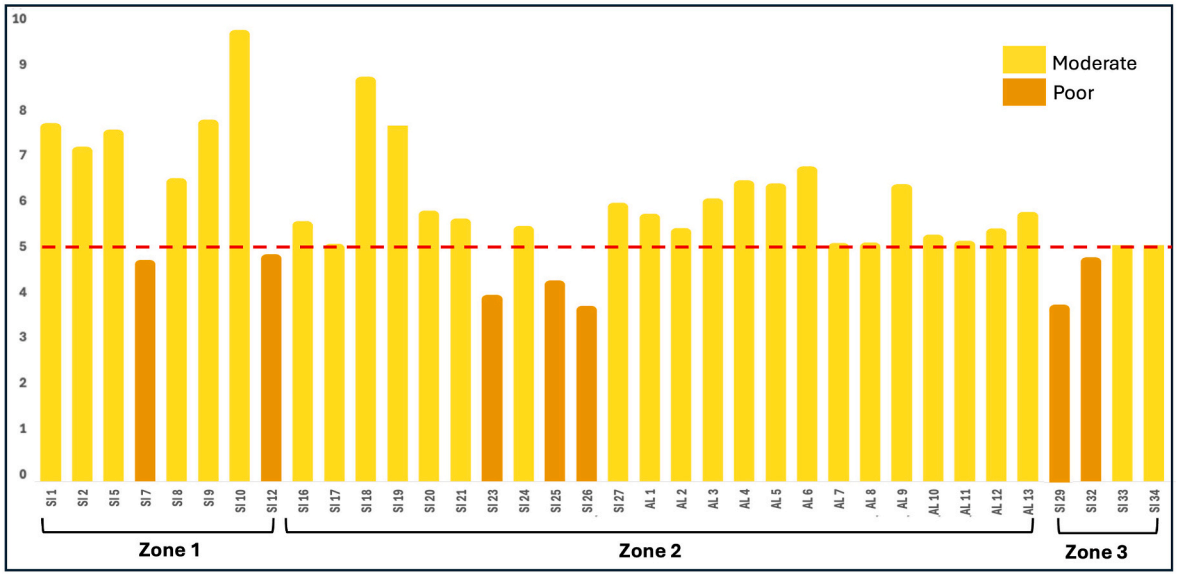


**Fig. 12.** Exponential of the bias-corrected Shannon diversity index (exp ($H'_{bc}$) across sampling sites. Bars are colored according to the ecological quality status (EcoQS). The dashed red line indicates the threshold value exp ($H'_{bc}$) = 5 used to distinguish between moderate and poor ecological quality (after Bouchet et al., 2012). (For interpretation of the references to color in this figure legend, the reader is referred to the Web version of this article).

values above 3, indicating a shift toward poor environmental quality, while SI5 and SI9 remained within the good category.

In Zone 2 (SI16 to SI26 and AL1 to AL13), the environmental quality was the most degraded, with the majority of sites classified as "Poor" or "Bad". Severely impacted sites include AL1, AL2, AL3, AL7, AL10, and AL12, while the remaining AL sites and several SI sites fell under the "Poor" Category. Only a few sites (e.g., SI17, SI18, SI20, SI21, SI24, SI27) maintained a "Moderate" status. In contrast to the exp ($H'_{bc}$) results, which indicated moderate diversity in this zone, the AMBI results highlighted a community dominated by opportunistic species, reflecting more intense anthropogenic disturbance. This divergence underscores the importance of using both structural and functional indicators in benthic assessments.

Zone 3 (SI31 to SI33) displayed relatively better conditions. Most sites fell within the good to moderate categories, with SI31 classified as unpolluted (AMBI 1.3). The highest AMBI value in Zone 3 was 4 at SI32, which is classified as poor, while SI33 remained moderate at 3. Overall, Zone 3 reflected environmental conditions more comparable to Zone 1, but with localized variability.

#### 4.7.4. Redundancy analysis (RDA)

The RDA model was statistically significant (permutation test, $p < 0.001$), explaining 60% of the variation in species–environment relationships (Fig. 14), indicating a strong influence of the selected environmental variables on the distribution of foraminiferal assemblages across the study area. In the first quadrant, sites from Zone 2 were predominantly grouped, with Al and suspended solids (turbidity) exhibiting the longest vectors, reflecting their dominant contribution to the species-environment associations in this sector of the ordination space. These sites were primarily associated with agglutinated species, including *Eggerella advena*, *Leptohalysis catella*, and *Textularia earlandi*.

In the second quadrant, sites belonging to Zone 1 and Zone 3 were clustered, strongly influenced by Si, quartz and sand. The corresponding species assemblages were dominated by calcareous taxa such as *Elphidium excavatum, Buccella frigida*, *Islandiella norcrossi*, and *Haynesina* sp.

In the third and fourth quadrants, additional sites from Zone 2 were distributed, corresponding to elevated concentrations of Fe and Mn, as well as high turbidity, silt, clay, and organic matter. The species associated with these gradients included *Spiroplectammina biformis*, *Ammotium cassis* and *Cribrostomoides* sp.

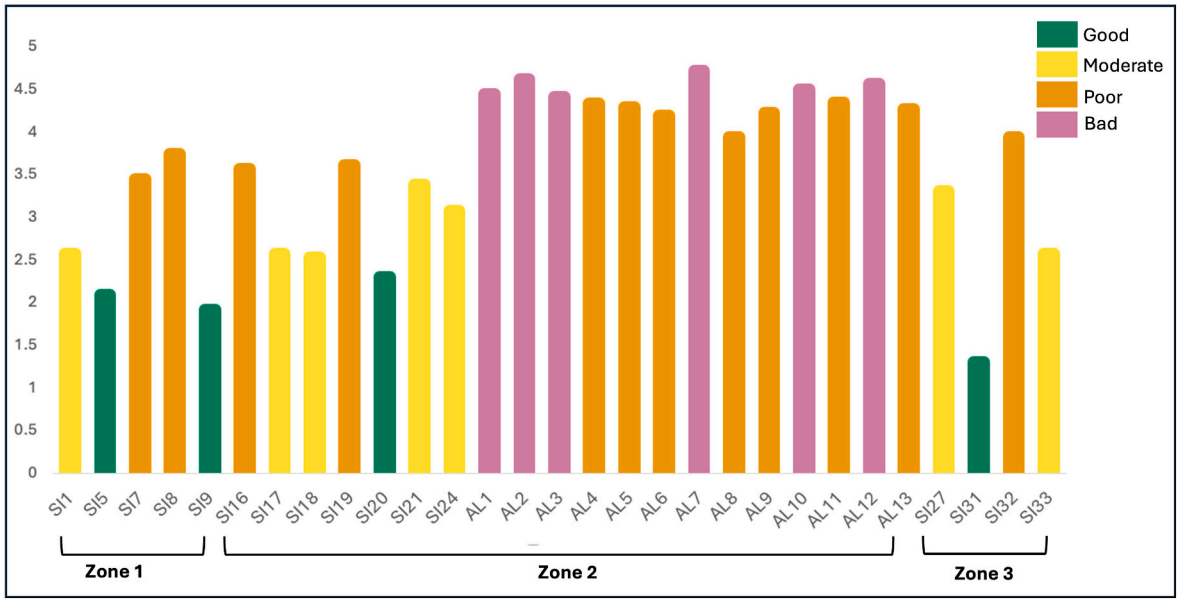


**Fig. 13.** Ecological Quality Status (EcoQS) across sampling sites based on the species-specific Foram-AMBI index.

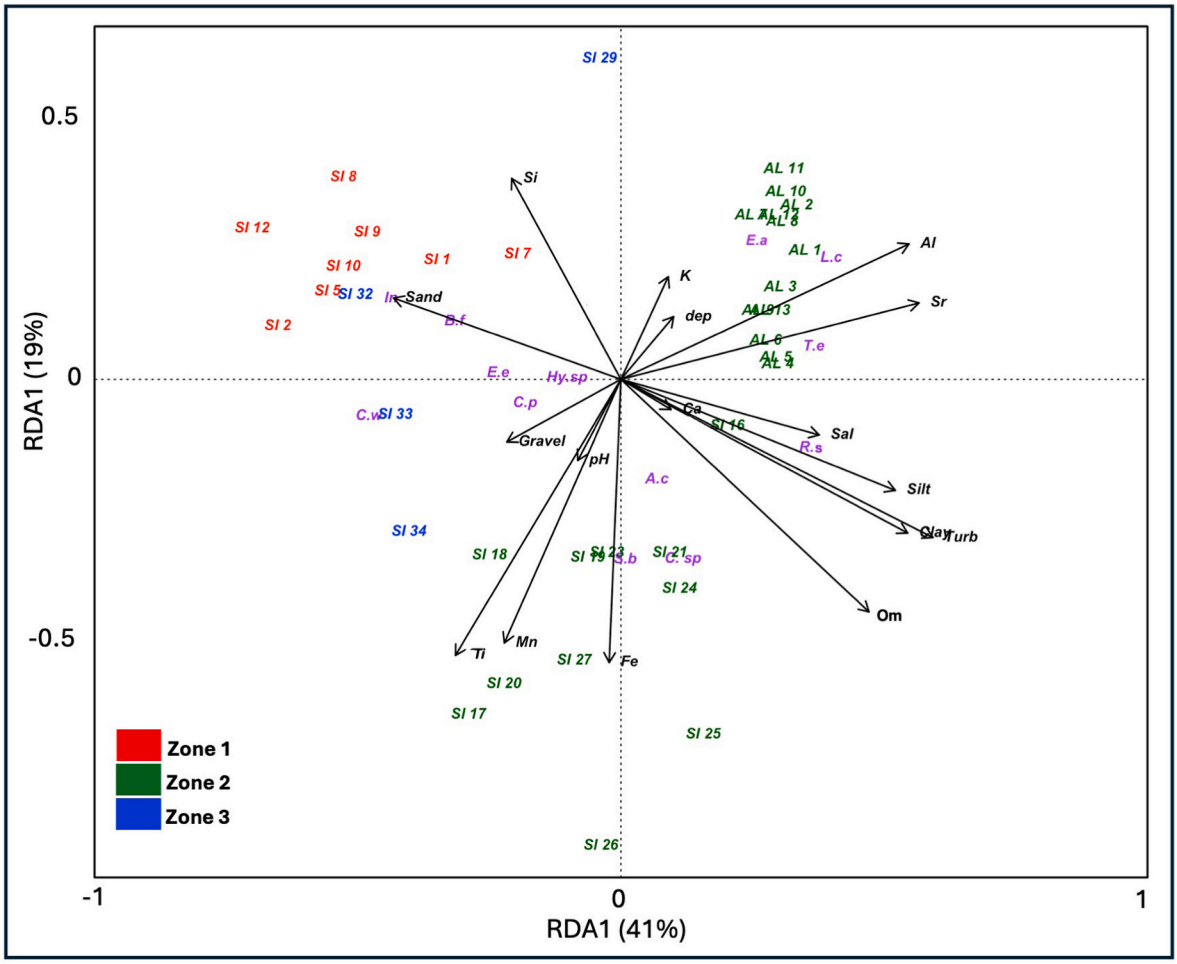


**Fig. 14.** Redundancy Analysis (RDA) of sites showing relationships between geochemical, mineralogical, foraminiferal, and granulometric data. *Ammotium cassis* (A. c), *Buccella frigida* (B.f), *Cibicidoides wuellerstorfi* (C.w), *Cornuspira planorbis* (C.p), *Cribrostomoides* sp. (C.sp), *Eggerella advena* (E.a), *Elphidium excavatum* (E.e), *Haynesina sp.* (Hy. sp), *Islandiella norcrossi* (I.n), *Leptohalysis catella* (L.c), *Reophax subfusiformis* (R.s), *Spiroplectammina biformis* (S.b), *Textularia earlandi* (T.e).

RDA separated agglutinated species, predominantly linked to Fe-rich and fine-grained environments, from the calcareous species, which were associated with quartz-rich, sandier environments. Sites within the bay were characterized by high Fe, clay, and OM levels, while sites outside the bay, particularly in Zone 1, were associated with sandier sediments.

## 5. Discussion

### *5.1. Sediment provenance and transport dynamics along the northern coast of the Gulf of St. Lawrence*

The sedimentary, mineralogical, and geochemical characteristics of the three zones: Port-Cartier, BSI, and Matamec highlight the diverse depositional settings and sediment-transport dynamics along the northern Gulf of St. Lawrence.

Zones 1 and 3 are dominated by coarse-grained sediments highlighting higher-energy conditions, likely due to their proximity to open water and stronger coastal currents, which limit the deposition of finer sediments (Savard et al., 2016). In contrast, Zone 2 exhibits a mixture of coarse and fine-grained sediments, with coarser materials dominating the eastern side and finer silt and clay accumulating toward the west. This distribution likely reflects a progressive reduction in current energy toward the western sector of the bay, allowing finer particles (e.g., silt, clay) to settle. The semi-enclosed nature of the bay, combined with the presence of the Sept-Îles Archipelago, influences current patterns and limits exchange with the open Gulf of St. Lawrence (Shaw et al., 2023). These conditions, along with localized currents and wave action, promote sediment redistribution toward the central part of the bay (Joshi et al., 2025). The linear westward movement of bottom currents, as described by Shaw et al. (2023), may further contribute to the westward transport and deposition of fine-grained material.

The compositional maturity of sediments along the northwestern Gulf of St. Lawrence is illustrated on the $SiO_2/Al_2O_3$ versus $Fe_2O_3/K_2O$ geochemical classification diagram (Herron, 1988), where samples cluster within the Shale–Wacke–Fe-Shale fields (Fig. 15A). This pattern indicates compositionally immature sediments with minimal recycling and limited sediment transport distances. Zone 1 exhibits a broad distribution across these fields, reflecting mixed felsic and intermediate sources, while Zone 2 clusters in the Fe-Shale field, highlighting contributions from oxide- and pyroxene-bearing mafic rocks. Zone 3 positions mainly between Wacke and Shale, consistent with reworking of Shield-derived material.

Complementing this, the discriminant diagram based on major elements developed in Roser and Korsch (1988), was used to infer sediment provenance in the BSI region (Fig. 15B). On this discrimination diagram most samples from all three zones plot between felsic and intermediate igneous provenance fields, confirming dominant inputs from granitoid and gneissic rocks of the Canadian Shield, together with material from the anorthositic and gabbroic units of the Sept-Îles Intrusive Suite (SIIS). A few samples from Zone 2 extend toward the mafic igneous field, consistent with the influence from gabbro-troctolite units of the Sept-Îles Intrusive Suite (SIIS).

Mineralogical data corroborate these geochemical trends. Zone 1 sediments near Port-Cartier contain abundant quartz, K-feldspar, and amphibole, reflecting erosion of local granitoid and metamorphic rocks (Fig. 16). The Aux-Rochers River acts as a primary conduit, delivering weathered Shield material to the coast, where sediment input is redistributed westward by littoral processes (Dredge, 2016; Shaw et al., 2023). Elevated Ca, K, Mg, and Zn concentrations further indicate contributions from mafic and ultramafic rocks rich in plagioclase.

In the BSI (Zone 2), sediment composition reflects both natural geological processes and anthropogenic activities (Dreujou et al., 2020). Rivers draining the SIIS (Figs. 1 and 2), including the des Rapides, Hall, au Foin, and du Poste rivers, deliver pyroxene and Fe–Ti oxides to the bay derived from gabbro-troctolite units, while coastal erosion of Proterozoic formations supplies quartz (Fig. 15). Consequently, iron is a major component of the bay sediments, largely inherited from Fe-Ti oxide-rich gabbro-troctolite layers of the SIIS. Recent findings by Joshi et al. (2025) indicate that anthropogenic activities have further increased iron concentrations in modern sediments. Indeed, Fe contents in a sediment core located at the entrance to the bay increase from ~4% at the base (pre-industrial reference) to ~6% at the top (post-industrial period), and the peaks in Fe and Fe-oxides in the upper core are consistent with historical industrial and mining contributions in the bay. Although the selected elements are commonly used as proxies for environmental quality in coastal systems with similar industrial settings (Souza et al., 2021), most concentrations remain close to regional or crustal background values, indicating a moderate low level of contamination.

Zone 3 (Matamec) sediments, supplied primarily by the Moisie River, exhibit high plagioclase and quartz contents, along with elevated Al, Ca, and Mg, indicating substantial contributions from anorthosite and mafic rocks such as gabbronorite and amphibolite (Fig. 15). These sediments are initially deposited in the Moisie delta, then transported westward by longshore drift along the coastal shelf toward the BSI sector (Normandeau et al., 2013).

Overall, these integrated geochemical and mineralogical observations demonstrate that sediment composition is primarily controlled by

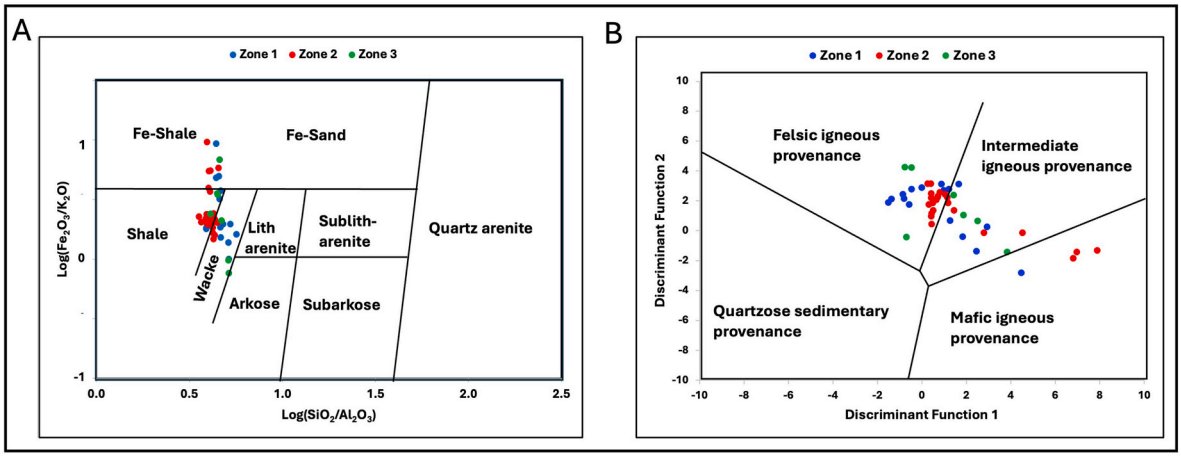


**Fig. 15.** Geochemical provenance classification diagrams. (A) Herron (1988) diagram based on Log ($SiO_2/Al_2O_3$) vs Log ($Fe_2O_3/K_2O$) for geochemical classification of sediments. (B) Discriminant-function plot of (Roser and Korsch, 1988) showing sediment-provenance fields.
(B) Discriminant-function plot of Roser and Korsch (1988) showing sediment-provenance fields.

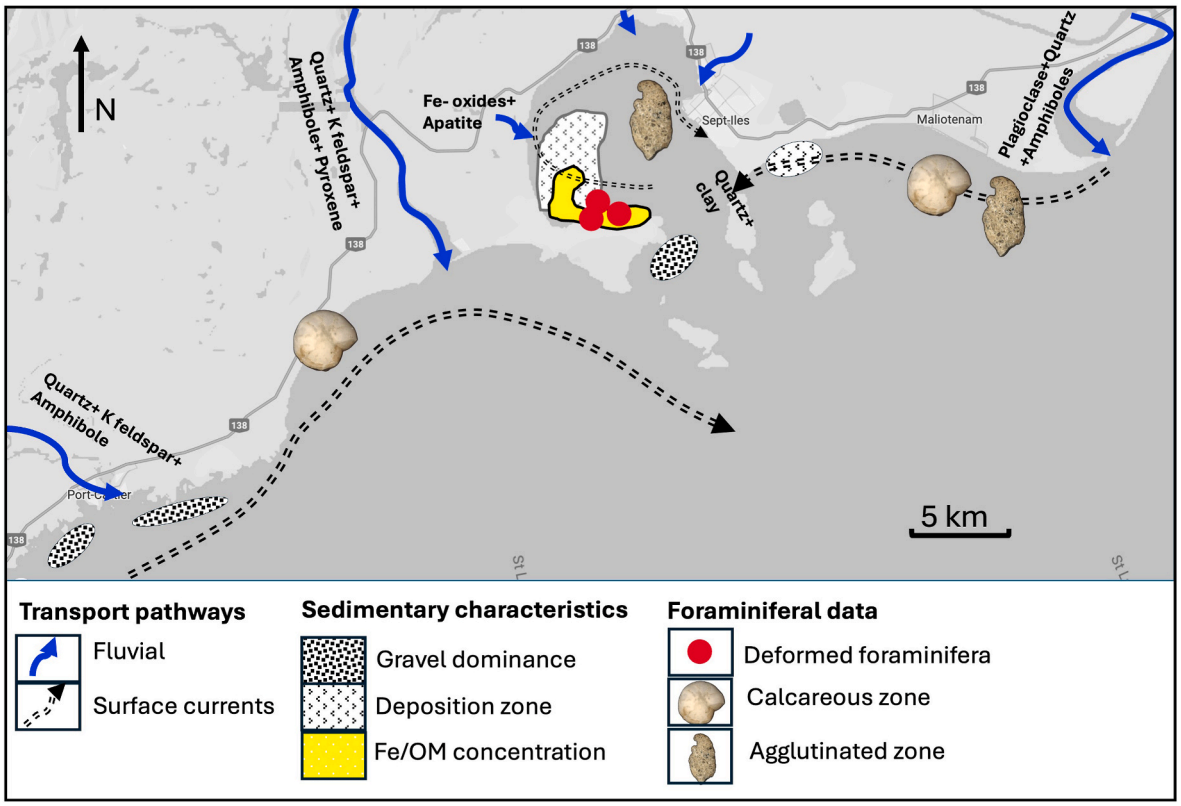


**Fig. 16.** Schematic map of the main sedimentary regions and transport pathways identified in the Gulf of St. Lawrence, specifically in the Port-Cartier, Bay of Sept-Îles, and Matamec areas. The map integrates surface current patterns (Shaw et al., 2023), sediment transport pathways including longshore drift (Normandeau et al., 2013; Joshi et al., 2025), and the dominant benthic foraminiferal assemblages observed in each zone.

local crystalline bedrock and nearshore transport processes, with limited long-distance sediment input.

### 5.2. *Spatial distribution patterns of benthic foraminifera are constrained by natural and anthropogenic environmental drivers*

The distribution patterns of foraminifera across the transect indicate that calcareous species such as *Cibicidoides wuellerstorfi* and *Buccella frigida* are primarily associated with silica-rich, coarse-grained sediments, typical of Zones 1 and 3. This observation is consistent with Venturelli et al. (2018), who reported that epifaunal taxa like *C. wuellerstorfi* thrive in environments where coarse sediments allow them to remain at or near the sediment–water interface. Their absence from Zone 2 highlights their sensitivity to environmental stressors, particularly elevated metal concentrations and organic enrichment. Notably, *C. wuellerstorfi* has also been identified as a highly sensitive species to pollution-related disturbances, such as oil spills, as shown in the study by Schwing and Machain-Castillo (2019). A comparable trend was observed in Halifax Harbour, where calcareous species initially disappeared due to chronic metal pollution, briefly returned following remediation, and subsequently vanished again as contamination persisted, giving way to opportunistic agglutinated forms (Mohamed, 2013). This mirrors the current scenario in the BSI, where agglutinated taxa dominate impacted sites, while calcareous taxa persist primarily in less disturbed zones. The redundancy analysis further clarifies these patterns where sites from Zone 2 cluster with Fe, Al, OM and turbidity, emphasizing their importance in structuring agglutinated assemblages, including species like *Eggerella advena*, *Leptohalysis catella*, *Spiroplectammina biformis*, *Ammotium cassis*, *Cribrostomoides* sp., and *Textularia earlandi*. Conversely, quartz and sand strongly influence sites from Zones 1 and 3, corresponding with the distribution of calcareous taxa such as *Elphidium excavatum*, *Buccella frigida*, *Islandiella norcrossi*, and *Haynesina* sp. This present-day dominance of agglutinated taxa aligns with historical reconstructions (Joshi et al., 2025), showing that shifts from calcareous to agglutinated assemblages coincide with industrial era increases in Fe, Mn, and OM. This indicates that current assemblage patterns may represent long-term responses to sustained environmental stress.

### 5.3. *Metal enrichment induced degraded ecological quality status in the Bay of Sept-îles*

The spatial variability observed through exp ($H'_{bc}$) and Foram-AMBI indices strongly aligns with the above-described abiotic gradients. Zone 1, characterized by moderate to high diversity and generally “Moderate” EcoQS values, corresponds to coarser, silica-rich sediments with lower concentrations of heavy metals, indicating relatively unpolluted conditions. In contrast, Zone 2 displays moderate diversity yet consistently poor to bad ecological quality according to the Foram-AMBI index, potentially reflecting stress linked to fine-grained sediments and high organic loading (Table S1). However, it should be noted that stress-tolerant foraminiferal taxa are naturally more abundant in fine-grained sediments, even in the absence of anthropogenic impact. A similar pattern was also found in O'Malley et al. (2021) that a site may have a high diversity (i.e. good or high EcoQS), as well as a high Foram-AMBI value (i.e. poor to bad EcoQS) due to a diverse assemblage of opportunistic species. The fact that exp ($H'_{bc}$) and Foram-AMBI do not point to the same EcoQS was already reported in previous studies (Al-Enezi et al., 2022; Cavaliere et al., 2021; El Kateb et al., 2020; Parent et al., 2021; Nunes et al., 2023). In contrast, Zone 3 shows a divergence

between EcoQS and Foram-AMBI results. While EcoQS values based on exp ($H'_{bc}$) classify most sites as "Poor" due to low diversity, the Foram-AMBI index indicates relatively better ecological conditions at some sites. This mismatch may be attributed to the naturally low foraminiferal abundance in this zone, associated with its coarse-grained sandy substrates that limit species richness and hinder assemblage development. The low diversity in Zone 3 is therefore not necessarily a signal of contamination but may instead reflect sampling limitations, especially where counts fell below the recommended threshold of 200 individuals per sample. In addition, the ecological group assignments used for the Foram-AMBI are derived from non-local reference datasets (North-East Atlantic). Ecological requirement of foraminiferal species may vary regionally leading to geographical variability in species assignments to ecological group as already observed in Europe i.e. the Atlantic coasts versus the Mediterranean Sea (Bouchet et al., 2021) and between Europe and Brazil (Bouchet et al., 2025). Therefore, the Foram-AMBI values presented here should be interpreted as relative indicators of environmental stress rather than absolute classifications. The lack of a region-specific species calibration represents a limitation of this study.

Conceptually, it is important to look at both species diversity and species-specific responses to environmental gradients when defining the quality of an area. Foram-AMBI is based on the response of species along a gradient of TOC, whereas exp ($H'_{bc}$) is based on the assemblages' diversity which is highly correlated with species richness. These findings emphasize the importance of considering both sedimentary context and foraminiferal abundance when interpreting diversity-based ecological assessments.

Foram-AMBI was originally developed for application to living foraminiferal assemblages. Therefore, some caution is needed in interpreting our results since we applied it to the total fauna (dead + living). However, the ecological quality status we observed is largely consistent with the measured abiotic parameters, suggesting that it may still provide meaningful ecological assessments when only total fauna is available.

Morphological deformities observed exclusively in specimens near the industrial area in the west further reflect the environmental stress, likely driven by elevated iron concentrations. Such deformities are consistent with previous studies. Polovodova and Schönfeld (2008) reported test abnormalities in benthic foraminifera linked to heavy metal pollution in the western Baltic Sea, while El-Kahawy et al. (2018) found similar deformities associated with metal contamination along the Red Sea coast. Experimental evidence has demonstrated that heavy metals, particularly Zn, can cause abnormal calcification, chamber arrangement, and aperture formation in foraminifera such as *Ammonia tepida* (Price et al., 2019). A comparable pattern has been documented in Halifax Harbour (Nova Scotia), where heavily polluted inner harbour environments were characterized by low-diversity assemblages dominated by non-calcareous taxa and high proportions of test deformities, whereas better flushed outer harbour areas contained diverse assemblages including calcareous species. Following improved wastewater treatment, the inner-harbour assemblages temporarily shifted toward calcareous dominated communities before reverting once treatment ceased (Dabbous and Scott, 2012). This study highlights the sensitivity of foraminiferal assemblages and deformities as rapid indicators of anthropogenic environmental stress. Another Long-term monitoring studies from North American estuaries further support the sensitivity of benthic foraminifera to anthropogenic stress. In Halifax Harbour and New Bedford Harbor, assemblages shifted from diverse, calcareous-dominated communities to low-diversity assemblages dominated by agglutinated taxa under increasing organic and industrial pollution, accompanied by high frequencies of test deformities (Scott et al., 2005). Although certain studies attribute test deformities to natural variations like salinity fluctuations (Stouff et al., 1999; Alve, 1995), stable salinity conditions recorded in Zone 2 reduce this likelihood, suggesting metal contamination as the primary stressor behind observed deformities.

Lastly, sites lacking foraminifera coincide consistently with areas dominated by high gravel content or active river deltas, environments characterized by strong currents and sediment reworking. These unstable substrates hinder colonization, providing minimal organic matter necessary for benthic foraminifera (Du Châtelet et al., 2009). Additionally, the porous gravel substrates facilitate increased water exchange, further limiting organic matter retention and the formation of essential low-oxygen microhabitats. Periodic freshwater influxes near river deltas, accompanied by fluctuating salinity and high suspended sediment loads, further compound these adverse conditions (Yanko-Hombach et al., 2017), rendering these areas inhospitable for sensitive foraminiferal species. This strongly suggests that the absence of foraminifera is linked to natural environmental impact rather than human induced.

## 6. Conclusion

This study integrates sedimentological, geochemical, and biological analyses to reveal the complex environmental dynamics of Port-Cartier, the BSI, and Matamec, in the northwestern Gulf of St. Lawrence. Distinct sedimentary conditions across these zones reflect interactions between local geology and hydrodynamic forces: high-energy environments at Port-Cartier and Matamec yield predominantly coarse sediments, while the BSI experiences variable energy conditions, resulting in a heterogeneous mix of fine and coarse sediments. Geochemical analyses highlight significant Fe enrichment within the BSI sediments, derived from natural geological sources and amplified by anthropogenic activities, leading to elevated iron and organic matter concentrations indicative of human influence.

Foraminiferal analysis demonstrates clear community differentiation aligned closely with these sedimentary and geochemical gradients. Calcareous species are notably absent from the BSI due to unfavorable conditions, including high iron concentrations, elevated turbidity, abundant organic matter, and fine-grained sediments. Conversely, agglutinated foraminifera dominate these Fe-rich, organic-laden sediments, showcasing their adaptability to stressful environmental conditions. High-energy river deltas and gravel-rich substrates further influence foraminiferal distributions, creating barren zones where substrate instability and sediment reworking prevent successful colonization. The clear spatial patterns observed through RDA provide quantitative validation of the relationship between sediment characteristics, metal enrichment, and community shifts.

These results underscore the value of integrating Foram-AMBI as sensitive ecological indicators to assess EcoQS, capable of detecting subtle anthropogenic disturbances in sub-Arctic estuarine environments. Additionally, documented morphological deformities in foraminifera serve as early warning bioindicators of environmental stress, even at contamination levels below regulatory thresholds.

As the first comprehensive foraminiferal study in this region, this research contributes valuable baseline data and bioindicator tools for long-term ecological monitoring. Importantly, the study enhances understanding of the sensitivity and adaptive responses of foraminiferal assemblages to both natural variability and anthropogenic pressures, informing future assessments of ecological health in northern coastal ecosystems.

## CRediT authorship contribution statement

**Neha Joshi:** Conceptualization, Formal analysis, Methodology, Validation, Visualization, Writing – original draft. **Jean-Carlos Montero-Serrano:** Funding acquisition, Investigation, Resources, Supervision, Validation, Writing – review & editing. **Vincent M.P. Bouchet:** Conceptualization, Investigation, Resources, Writing – review & editing. **Emilie Arseneault:** Validation, Writing – review & editing. **Émilie Saulnier-Talbot:** Conceptualization, Funding acquisition,

Investigation, Resources, Supervision, Validation, Writing – review & editing.

## Declaration of competing interest

The authors declare that they have no known competing financial interests or personal relationships that could have appeared to influence the work reported in this paper.

## Acknowledgements

This research was supported by: Université Laval EcoZone research Chair in partnership with the Port of Sept-Îles and INREST; the RQM through the Odyssée Saint-Laurent research program; the Natural Sciences and Engineering Research Council of Canada (NSERC) through Discovery Grants provided to É. Saulnier-Talbot and J.-C. Montero-Serrano; and the FRQ, Québec Océan Strategic Cluster. This work benefited from the technical support of the EMIMA experimental platform from Université de Lille. Finally, we thank the two anonymous reviewers for their constructive feedback, which improved the quality of the manuscript, and Steve Mitchell (University of Portsmouth) for his editorial support.

## Appendix A. Supplementary data

Supplementary data to this article can be found online at https://doi.org/10.1016/j.ecss.2026.109828.

## Data availability

Following acceptance, all relevant datasets will be archived and made accessible through the Borealis research data repository.

## References

Ahmadi-Nedushan, B., St-Hilaire, A., Ouarda, T.B., Bilodeau, L., Robichaud, E., Thiémonge, N., Bobée, B., 2007. Predicting river water temperatures using stochastic models: case study of the Moisie River (Québec, Canada). Hydrol. Process. 21, 21–34. https://doi.org/10.1002/hyp.6167.

Al-Enezi, E., Francescangeli, F., Balassi, E., Borderie, S., Al-Hazeem, S., Salamin, F., Boota, A.A., Pawlowski, J., Frontalini, F., 2022. Benthic foraminifera as proxies for the environmental quality assessment of the Kuwait Bay (Kuwait, Arabian Gulf): morphological and metabarcoding approaches. Sci. Total Environ. 833, 155093. https://doi.org/10.1016/j.scitotenv.2022.155093.

Alldred, F.C., Gröcke, D.R., Jackson, S.E., Reid, G., 2024. Nitrogen isotopes in herbaria document historical nitrogen sewage pollution in the Mersey Estuary, England. Environ. Sci. Adv. 3, 676–685. https://doi.org/10.1039/D4VA00033A.

Alve, E., 1995. Benthic foraminiferal responses to estuarine pollution: a review. J. Foraminifer. Res. 25, 190–203. https://doi.org/10.2113/gsjfr.25.3.190.

Alve, E., 2003. A common opportunistic foraminiferal species as an indicator of rapidly changing conditions in a range of environments. Estuar. Coast Shelf Sci. 57, 501–514. https://doi.org/10.1016/S0272-7714(02)00396-2.

Alve, E., Korsun, S., Schönfeld, J., Dijkstra, N., Golikova, E., Hess, C., Husum, K., Panieri, G., 2016. Foram-AMBI: a sensitivity index based on benthic foraminiferal faunas from North-East Atlantic and Arctic fjords, continental shelves and slopes. Mar. Micropaleontol. 122, 1–12. https://doi.org/10.1016/j.marmicro.2015.11.001.

Alve, E., Lepland, A., Magnusson, J., Backer-Owe, K., 2009. Monitoring strategies for re-establishment of ecological reference conditions: possibilities and limitations. Mar. Pollut. Bull. 59, 297–310. https://doi.org/10.1016/j.marpolbul.2009.08.015.

Barras, C., Jorissen, F.J., Labrune, C., Andral, B., Boissery, P., 2014. Live benthic foraminiferal faunas from the French mediterranean coast: towards a new biotic index of environmental quality. Ecol. Indic. 36, 719–733. https://doi.org/10.1016/j.ecolind.2013.09.019.

Blott, S.J., Pye, K., 2001. GRADISTAT: a grain size distribution and statistics package for the analysis of unconsolidated sediments. Earth Surf. Process. Landf. 26, 1237–1248. https://doi.org/10.1002/esp.261.

Bouchet, V.M., Sousa, S.H.D.M.E., Bonetti, C., Burone, L., Belart, P., Duleba, W., Francescangeli, F., Frontalini, F., Laut, L., Raposo, D.S., Rodrigues, A.R., 2025. Towards a more integrative approach for environmental decision-making in Brazilian transitional waters: improving biomonitoring surveys with a benthic foraminiferal biotic index. J. Micropalaeontol. 44 (2), 237–261.

Bouchet, V.M.P., Alve, E., Rygg, B., Telford, R.J., 2012. Benthic Foraminifera provide a promising tool for ecological quality assessment of marine waters. Ecol. Indic. 23, 66–75. https://doi.org/10.1016/j.ecolind.2012.03.013.

Bouchet, V.M.P., Frontalini, F., Francescangeli, F., Sauriau, P.-G., Geslin, E., Martins, M. V.A., Almogi-Labin, A., Avnaim-Katav, S., Di Bella, L., Cearreta, A., Coccioni, R., Costelloe, A., Dimiza, M.D., Ferraro, L., Haynert, K., Martinez-Colon, M., Melis, R., Schweizer, M., Triantaphyllou, M., Tsujimoto, A., Wilson, B., Armynot du Châtelet, E., 2021. Indicative value of benthic foraminifera for biomonitoring: assignment to ecological groups of sensitivity to total organic carbon of species from European intertidal areas and transitional waters. Mar. Pollut. Bull. 164, 112071. https://doi.org/10.1016/j.marpolbul.2021.112071.

Bouchet, V.M.P., Goberville, E., Frontalini, F., 2018. Benthic foraminifera to assess the ecological quality status of Italian transitional waters. Ecol. Indic. 84, 130–139. https://doi.org/10.1016/j.ecolind.2017.08.049.

Bouchet, V., Seuront, L., 2020. Strength may lie in numbers: intertidal foraminifera non-negligible contribution to surface sediment reworking. Open J. Mar. Sci. 10, 131–140. https://doi.org/10.4236/ojms.2020.103010.

Butler, B.M., Hillier, S., 2021. powdR: an R package for quantitative mineralogy using full pattern summation of X-ray powder diffraction data. Comput. Geosci. 147, 104662. https://doi.org/10.1016/j.cageo.2020.104662.

Carrière, J., Le Hénaff, A., 2018. Mise en contexte. Rapport global sur l'observatoire environnemental de la baie de Sept-Îles 1, 35–42. Available at: https://inrest.ca/wp-content/uploads/2021/04/Livre-COMPLET-INREST.pdf. (Accessed 6 November 2024).

Cavaliere, M., Barrenechea, I., Montresor, M., Bucci, C., Brocani, L., Balassi, E., Margiotta, F., Francescangeli, F., Bouchet, V.M.P., Pawlowski, J., Frontalini, F., 2021. Assessing the ecological quality status of the highly polluted Bagnoli area (Tyrrhenian Sea, Italy) using foraminiferal eDNA metabarcoding. Sci. Total Environ. 790, 147871. https://doi.org/10.1016/j.scitotenv.2021.147871.

Choquel, C., Geslin, E., Metzger, E., Filipsson, H.L., Risgaard-Petersen, N., Launeau, P., Giraud, M., Jauffrais, T., Jesus, B., Mouret, A., 2021. Denitrification by benthic foraminifera and their contribution to N-loss from a fjord environment. Biogeosciences 18, 327–341. https://doi.org/10.5194/bg-18-327-2021.

Chronopoulou, P.M., Salonen, I., Bird, C., Reichart, G.J., Koho, K.A., 2019. Metabarcoding insights into the trophic behavior and identity of intertidal benthic foraminifera. Front. Microbiol. 10, 1169. https://doi.org/10.3389/fmicb.2019.01169.

Dabbous, S.A., Scott, D.B., 2012. Short-term monitoring of Halifax Harbour (Nova Scotia, Canada) pollution remediation using benthonic foraminifera as proxies. J. Foraminifer. Res. 42 (3), 187–205.

de Vernal, A., Henry, M., Bilodeau, G., 1999. Techniques de préparation et d'analyse en micropaléontologie. Les Cahiers du GEOTOP 3, 41.

Deldicq, N., Langlet, D., Delaeter, C., Beaugrand, G., Seuront, L., Bouchet, V.M., 2021a. Effects of temperature on the behaviour and metabolism of an intertidal foraminifera and consequences for benthic ecosystem functioning. Sci. Rep. 11, 4013. https://doi.org/10.1038/s41598-021-83561-8.

Deldicq, N., Seuront, L., Bouchet, V.M.P., 2021b. Inter-specific and inter-individual trait variability matter in surface sediment reworking rates of intertidal benthic foraminifera. Mar. Biol. 168, 101. https://doi.org/10.1007/s00227-021-03908-w.

Desrosiers, C., Leflaive, J., Eulin, A., Ten-Hage, L., 2013. Bioindicators in marine waters: benthic diatoms as a tool to assess water quality from eutrophic to oligotrophic coastal ecosystems. Ecol. Indic. 32, 25–34. https://doi.org/10.1016/j.ecolind.2013.03.028.

Dredge, L.A., 2016. Quaternary Geomorphology of the Quebec North Shore, Godbout to Sept-Îles, 8136. Geological Survey of Canada, p. 28. https://doi.org/10.4095/297857.

Dreujou, E., McKindsey, C.W., Grant, C., Tréau de Coeli, L., St-Louis, R., Archambault, P., 2020. Biodiversity and habitat assessment of coastal benthic communities in a sub-Arctic industrial harbor area. Water 12, 2424. https://doi.org/10.3390/w12092424.

Du Châtelet, É.A., Bout-Roumazeilles, V., Riboulleau, A., Trentesaux, A., 2009. Sediment (grain size and clay mineralogy) and organic matter quality control on living benthic foraminifera. Rev. Micropaleontol. 52, 75–84. https://doi.org/10.1016/j.revmic.2008.10.003.

Du Châtelet, É.A., Debenay, J.P., Soulard, R., 2004. Foraminiferal proxies for pollution monitoring in moderately polluted harbors. Environ. Pollut. 127, 27–40. https://doi.org/10.1016/j.envpol.2003.07.002.

El Kateb, A., Stalder, C., Martinez-Colón, M., Mateu-Vicens, G., Francescangeli, F., Coletti, G., StainbanK, S., Spezzaferri, S., 2020. Foraminiferal-based biotic indices to assess the ecological quality status of the Gulf of Gabes (Tunisia): present limitations and future perspectives. Ecol. Indic. 111, 105962. https://doi.org/10.1016/j.ecolind.2019.105962.

El-Kahawy, R., El-Shafeiy, M., Helal, S.A., Aboul-Ela, N., Abd El-Wahab, M., 2018. Morphological deformities of benthic foraminifera in response to nearshore pollution of the Red Sea, Egypt. Environ. Monit. Assess. 190, 312. https://doi.org/10.1007/s10661-018-6632-5.

Francescangeli, F., Du Chatelet, E.A., Billon, G., Trentesaux, A., Bouchet, V.M.P., 2016. Palaeo-ecological quality status based on foraminifera of Boulogne-sur-Mer harbour (Pas-de-Calais, Northeastern France) over the last 200 years. Mar. Environ. Res. 117, 32–43. https://doi.org/10.1016/j.marenvres.2016.04.007.

Francescangeli, F., Quijada, M., Armynot du Châtelet, E., Frontalini, F., Trentesaux, A., Billon, G., Bouchet, V.M.P., 2020. Multidisciplinary study to monitor consequences of pollution on intertidal benthic ecosystems (Hauts de France, English Channel, France): comparison with natural areas. Mar. Environ. Res. 160, 105034. https://doi.org/10.1016/j.marenvres.2020.105034.

Gamboa, A., Montero-Serrano, J.C., St-Onge, G., Rochon, A., Desiage, P.A., 2017. Mineralogical, geochemical, and magnetic signatures of surface sediments from the Canadian Beaufort Shelf and Amundsen Gulf (Canadian Arctic). G-cubed 18, 488–512. https://doi.org/10.1002/2016GC006449.

Glock, N., Richirt, J., Woehle, C., Algar, C., Armstrong, M., Eichner, D., Firrincieli, H., Govindankutty Menon, A., Ishitani, Y., Hackl, T., Hubert-Huard, R., 2025. Widespread occurrence of phosphate storage in foraminifera: adaption to $O_2$ depletion and relevance for P-cycling. Nature 638, 1000–1006.
Gouvernement du Québec, ministère de l'Environnement et de la Lutte contre les changements climatiques, Direction des aires protégées, 2022. Réserve Écologique de la Matamec. Plan de Conservation. Gouvernement du Québec, Québec.
Government of Canada, 2024. Tides, currents, and water levels. Available at: https://tides.gc.ca/en/stations/2790. (Accessed 6 November 2024).
Hayward, B.W., Le Coze, F., Vachard, D., Gross, O., 2024. World Foraminifera database. Available at: https://www.marinespecies.org/foraminifera. (Accessed 6 November 2024) https://doi.org/10.14284/305.
He, Q., Silliman, B.R., 2019. Climate change, human impacts, and coastal ecosystems in the Anthropocene. Curr. Biol. 29, R1021–R1035. https://doi.org/10.1016/j.cub.2019.08.042.
Heiri, O., Lotter, A.F., Lemcke, G., 2001. Loss on ignition as a method for estimating organic and carbonate content in sediments: reproducibility and comparability of results. J. Paleolimnol. 25, 101–110. https://doi.org/10.1023/A:1008119611481.
Herron, M.M., 1988. Geochemical classification of terrigenous sands and shales from core or log data. J. Sediment. Petrol. 58, 820–829.
Higgins, M.D., 2005. A new interpretation of the structure of the Sept Îles Intrusive Suite, Canada. Lithos 83, 199–213. https://doi.org/10.1016/j.lithos.2005.01.004.
Humphreys, A.F., Halfar, J., Ingle, J.C., Manzello, D., Reymond, C.E., Westphal, H., Riegl, B., 2018. Effect of seawater temperature, pH, and nutrients on the distribution and character of low abundance shallow water benthic Foraminifera in the Galápagos. PLoS One 13, e0202746. https://doi.org/10.1371/journal.pone.0202746.
INREST, 2016. Environmental observatory for the Bay of sept-Îles – work on phase II begins. Available at: https://inrest.ca/wp-content/uploads/2020/01/Observatoire-de-veille-environnementale-de-la-baie-de-Sept-I%CC%82les-Pre%CC%81sentation-du-rapport-de-la-phase-II-%E2%80%93-Port-de-Sept-I%CC%82les.pdf. (Accessed 6 November 2024).
INREST, 2018. Environmental observatory for the Bay of Sept-Îles – presentation of overall report. Available at: https://inrest.ca/wp-content/uploads/2020/01/5-Environmental-Observatory-for-the-Bay-of-Sept-I%CC%82les-%E2%80%93-Presentation-of-overall-report-%E2%80%93-Port-de-Sept-I%CC%82les.pdf. (Accessed 6 November 2024).
Jauffrais, T., LeKieffre, C., Schweizer, M., Geslin, E., Metzger, E., Bernhard, J.M., Jesus, B., Filipsson, H.L., Maire, O., Meibom, A., 2019. Kleptoplastidic benthic foraminifera from aphotic habitats: insights into assimilation of inorganic C, N and S studied with sub-cellular resolution. Environ. Microbiol. 21, 125–141. https://doi.org/10.1111/1462-2920.14434.
Jorissen, F.J., Nardelli, M.P., Almogi-Labin, A., Barras, C., Bergamin, L., Bicchi, E., El Kateb, A., Ferraro, L., McGann, M., Morigi, C., Romano, E., Sabbatini, A., Schweizer, M., Spezzaferri, S., 2018. Developing Foram-AMBI for biomonitoring in the mediterranean: species assignments to ecological categories. Mar. Micropaleontol. 140, 33–45. https://doi.org/10.1016/j.marmicro.2017.12.006.
Joshi, N., Montero-Serrano, J.C., Lefebvre, C., Saulnier-Talbot, É., 2025. Tracking pre- and post-industrialization changes in the Bay of Sept-Îles (Canada) using foraminifera as bioindicators. J. Coast Res. 41, 255–271. https://doi.org/10.2112/JCOASTRES-D-24A-00009.1.
Alboukadel, Kassambara, Fabian, Mundt, factoextra: Extract and Visualize the Results of Multivariate Data Analyses, CRAN: Contributed Packages, 2016, 10.32614/cran.package.factoextra, https://CRAN.R-project.org/package=factoextra, The R Foundation.
Kennish, M.J., 2002. Environmental threats and environmental future of estuaries. Environ. Conserv. 29, 78–107. https://doi.org/10.1017/S0376892902000061.
Lê, Sébastien, Josse, Julie, Husson, François, 2008. FactoMineR: A Package for Multivariate Analysis. Journal of Statistical Software 25 (1). https://doi.org/10.18637/jss.v025.i01. http://www.jstatsoft.org/v25/i01/, 2008.
Lajeunesse, P., St-Onge, G., Labbé, G., Locat, J., 2007. Morphosedimentology of submarine mass-movements and gravity flows offshore Sept-Îles, NW Gulf of St. Lawrence (Québec, Canada). In: Lykousis, V., Sakellariou, D., Locat, J. (Eds.), Submarine Mass Movements and Their Consequences. Springer, Berlin, pp. 287–296. https://doi.org/10.1007/978-1-4020-6512-5_32.
Langlet, D., Mermillod-Blondin, F., Deldicq, N., Bauville, A., Duong, G., Konecny, L., Hugoni, M., Denis, L., Bouchet, V.M., 2023. Single-celled bioturbators: benthic foraminifera mediate oxygen penetration and prokaryotic diversity in intertidal sediment. Biogeosciences 20, 4875–4891. https://doi.org/10.5194/bg-20-4875-2023.
Lapointe, M., 2000. Modern diatom assemblages in surface sediments from the maritime estuary and the Gulf of St. Lawrence, Québec (Canada). Mar. Micropaleontol. 40, 43–65. https://doi.org/10.1016/S0377-8398(00)00006-8.
Lee, G.H., Jung, N., Dellapenna, T., Ra, K., Chang, J., Kong, G.S., Jeong, H., 2024. Pace of heavy metal pollution in the anthropogenically altered and industrialized Nakdong River Estuary, South Korea: implications for the Anthropocene. Mar. Pollut. Bull. 205, 116678. https://doi.org/10.1016/j.marpolbul.2023.116678.
Lee, Y.G., Kim, S., Kim, Y.W., Jeong, D.U., Lee, J.S., Woo, H.J., Shin, H.C., 2015. Benthic foraminifera as bioindicators of salinity variation in Lake Shihwa, South Korea. J. Foraminifer. Res. 45 (3), 235–249.
Loeblich, A.R., Tappan, H., 1987. Foraminiferal Genera and their Classification. Van Nostrand Reinhold, New York, p. 970.
Lotze, H.K., Lenihan, H.S., Bourque, B.J., Bradbury, R.H., Cooke, R.G., Kay, M.C., Kidwell, S.M., Kirby, M.X., Peterson, C.H., Jackson, J.B., 2006. Depletion, degradation, and recovery potential of estuaries and coastal seas. Science 312, 1806–1809. https://doi.org/10.1126/science.1128035.
Marine Link, 2024. Port-cartier information. Available at: https://ports.marinelink.com/ports/port/port-cartier. (Accessed 6 November 2024).
Mohamed, S.A., 2013. Monitoring of the Remediation of Halifax Harbour after 250 Years of Contamination Using Foraminiferal Proxies. PhD thesis. Dalhousie University, Halifax. Available at: https://dalspace.library.dal.ca/handle/10222/21692. (Accessed 6 November 2024).
Mojtahid, M., Jorissen, F., Durrieu, J., Galgani, F., Howa, H., Redois, F., Camps, R., 2006. Benthic foraminifera as bio-indicators of drill cutting disposal in tropical east Atlantic outer shelf environments. Mar. Micropaleontol. 61, 58–75. https://doi.org/10.1016/j.marmicro.2006.05.003.
Moodley, L., Boschker, H.T.S., Middelburg, J.J., Pel, R., Herman, P.M.J., De Deckere, E. M.G.T., Heip, C.H.R., 2000. Ecological significance of benthic foraminifera: $^{13}C$ labelling experiments. Mar. Ecol. Prog. Ser. 202, 289–295. https://doi.org/10.3354/meps202289.
Murray, J.W., 2006. Ecology and Applications of Benthic Foraminifera. Cambridge University Press, Cambridge, p. 426.
Namur, O., Higgins, M.D., Vander Auwera, J., 2015. The Sept iles intrusive suite, Quebec, Canada. In: Charlier, B., Namur, O., Latypov, R., Tegner, C. (Eds.), Layered Intrusions. Springer, Dordrecht, pp. 465–515. https://doi.org/10.1007/978-94-017-9652-1_12.
Nomaki, H., Ogawa, N.O., Ohkouchi, N., Suga, H., Toyofuku, T., Shimanaga, M., Nakatsuka, T., Kitazato, H., 2008. Benthic foraminifera as trophic links between phytodetritus and benthic metazoans: carbon and nitrogen isotopic evidence. Mar. Ecol. Prog. Ser. 357, 153–164. https://doi.org/10.3354/meps07309.
Normandeau, A., Lajeunesse, P., St-Onge, G., 2013. Shallow-water longshore drift-fed submarine fan deposition (Moisie River Delta, Eastern Canada). Geo Mar. Lett. 33, 391–403. https://doi.org/10.1007/s00367-013-0338-6.
Nunes, M., Martins, M.V.A., Frontalini, F., Bouchet, V.M., Francescangeli, F., Hohenegger, J., Figueira, R., Senez-Mello, T.M., Castelo, W.F.L., Damasceno, F.L., Laut, L., 2023. Inferring the ecological quality status based on living benthic foraminiferal indices in transitional areas of the Guanabara Bay (SE Brazil). Environ. Pollut. 320, 121003. https://doi.org/10.1016/j.envpol.2023.121003.
O'Brien, P., Polovodova Asteman, I., Bouchet, V.M.P., 2021. Benthic foraminiferal indices and environmental quality assessment of transitional waters: a review of current challenges and future research perspectives. Water 13, 1898. https://doi.org/10.3390/w13131898.
O'Malley, B.J., Schwing, P.T., Martínez-Colón, M., Spezzaferri, S., Machain-Castillo, M.L., Larson, R.A., Brooks, G.R., Ruiz-Fernández, A.C., Hollander, D.J., 2021. Development of a benthic foraminifera based marine biotic index (Foram-AMBI) for the Gulf of Mexico: a decision support tool. Ecol. Indic. 120, 106916. https://doi.org/10.1016/j.ecolind.2020.106916.
OBV Saguenay, 2015. Fiche-portrait – bassin versant de la rivière Sainte-Marguerite. Organisme de Bassins Versants du Saguenay. Available at:, Section 2.1.2.6.8. https://www.obvsaguenay.org/wp-content/uploads/2020/09/pdesaguenay2015doc04-0_portraitchap2_obvs2015.pdf. (Accessed 6 November 2024).
OBVD (Organisation de bassins versants du domaine de la rivière aux Rochers), 2019a. Portrait du Bassin versant Aux Rochers. Available at: https://obvd.qc.ca/fiches-portraits/riviere-aux-rochers/fiche-portrait.pdf. (Accessed 6 November 2024).
OBVD (Organisme de bassins versants Duplessis), 2019b. Fiche-portrait – rivière des Rapides. Sept-Îles, Québec. Available at: https://obvd.qc.ca/fiches-portraits/riviere-des-rapides/fiche-portrait.pdf. (Accessed 6 November 2024).
Oksanen, J., Blanchet, F.G., Friendly, M., Kindt, R., Legendre, P., McGlinn, D., Minchin, P.R., O'Hara, R.B., Simpson, G.L., Solymos, P., Stevens, M.H.H., Szoecs, E., Wagner, H., 2020. Vegan: community ecology package. R package version 2, 5–7.
Parent, B., Barras, C., Bicchi, E., Charrieau, L.M., Choquel, C., Bénéteau, É., Maillet, G.M., Jorissen, F.J., 2021. Comparison of four foraminiferal biotic indices assessing the environmental quality of coastal Mediterranean soft bottoms. Water 13 (22), 3193. https://doi.org/10.3390/w13223193.
Piña-Ochoa, E., Hogslund, S., Geslin, E., Cedhagen, T., Revsbech, N.P., Nielsen, L.P., Schweizer, M., Jorissen, F., Rysgaard, S., Risgaard-Petersen, N., 2010. Widespread occurrence of nitrate storage and denitrification among Foraminifera and Gromiida. Proc. National Acad. Sci. USA 107, 1148–1153. https://doi.org/10.1073/pnas.0908440107.
Plan Saint-Laurent, 2024. Overview of the State of the St. Lawrence – 2024 (Portrait Global 2024). Government of Canada and Government of Québec. Available at: https://www.planstlaurent.qc.ca/en/developing-knowledge/overview-of-the-state-of-the-st-lawrence/translate-to-english-portrait-global-2024. (Accessed 6 November 2024).
Polovodova, I., Schönfeld, J., 2008. Foraminiferal test abnormalities in the western Baltic sea. J. Foraminifer. Res. 38, 318–336. https://doi.org/10.2113/gsjfr.38.4.318.
Port of Sept-Îles, n.d. Environmental observatory for the Bay of Sept-Îles. Available at: https://www.portsi.com/environment/environmental-observatory-for-the-bay-of-sept-iles/?lang=en (accessed 6 November 2024).
Price, E.B., Kabengi, N., Goldstein, S.T., 2019. Effects of heavy-metal contaminants (Cd, Pb, Zn) on benthic foraminiferal assemblages grown from propagules, Sapelo Island, Georgia (USA). Mar. Micropaleontol. 147, 1–11. https://doi.org/10.1016/j.marmicro.2019.01.001.
QGIS Development Team, 2024. *QGIS Geographic Information System* (Version 3.34). Open Source Geospatial Foundation Project. Available at: https://qgis.org. (Accessed 6 November 2024).
R Core Team, 2023. R: a Language and Environment for Statistical Computing. R Foundation for Statistical Computing, Vienna. Available at: https://www.r-project.org. (Accessed 13 May 2024).
Rodrigues, C.G., 1980. Holocene Microfauna and Paleoceanography of the Gulf of St. Lawrence. PhD Thesis. Carleton University, Ottawa.

Roser, B.P., Korsch, R.J., 1988. Provenance signatures of sandstone-mudstone suites determined using discriminant function analysis of major-element data. Chem. Geol. 67 (1-2), 119–139.

Sambugaro, J., Kropiwiec, I.S., Pereira, L.G., Sarmiento, J.A.S., Magalhães, R.H., Siegle, E., Figueira, R.C.L., Martins, M.V.A., Bouchet, V.M., Frontalini, F., de Sousa, S.H.M., 2025. Contrasting natural and anthropic historical changes in two estuarine systems on the Brazilian coast: benthic foraminiferal-based Paleo-ecological quality status. Mar. Environ. Res., 107306 https://doi.org/10.1016/j.marenvres.2025.107306.

Savard, J.-P., van Proosdij, D., O'Carroll, S., 2016. Perspectives on Canada's East Coast region. In: Lemmen, D.S., Warren, F.J., James, T.S., Mercer Clarke, C.S.L. (Eds.), Canada's Marine Coasts in a Changing Climate. Government of Canada, Ottawa, pp. 99–152.

Philipp, Schauberger, Alexander, Walker, openxlsx: Read, Write and Edit xlsx Files, CRAN: Contributed Packages, 2014, 10.32614/cran.package.openxlsx, https://CRAN.R-project.org/package=openxlsx, The R Foundation.

Schwing, P.T., Machain-Castillo, M.L., 2019. Impact and resilience of benthic foraminifera in the aftermath of the deepwater horizon and ixtoc 1 oil spills. In: Murawski, S.A., Ainsworth, C.H., Paris, C.B., Peebles, E.B., Greer, C.W. (Eds.), Deep Oil Spills: Facts, Fate, and Effects. Springer, Cham, pp. 374–387. https://doi.org/10.1007/978-3-030-11605-7_20.

Scott, D.B., Tobin, R., Williamson, M., Medioli, F.S., Latimer, J.S., Boothman, W.A., Asioli, A., Haury, V., 2005. Pollution monitoring in two North American estuaries: historical reconstructions using benthic foraminifera. J. Foraminifer. Res. 35 (1), 65–82.

Shaw, J.-L., Bourgault, D., Dumont, D., Lefaivre, D., 2023. Hydrodynamics of the Bay of Sept-Îles. Atmos.-Ocean 61, 105–121. https://doi.org/10.1080/07055900.2022.2094791.

Souza, A.H.D., Krüger, F.L.V., Araújo, F.G.D.S., Mendes, J.J., 2021. Mineralogical characterization applied to iron ore tailings from the desliming stage with emphasis on quantitative electron microscopy (Qem). Mater. Res. 24, e20190677.

Stouff, V., Geslin, E., Debenay, J.P., Lesourd, M., 1999. Origin of morphological abnormalities in *Ammonia* (Foraminifera): studies in laboratory and natural environments. J. Foraminifer. Res. 29, 152–170. https://doi.org/10.2113/gsjfr.29.2.152.

Stuhr, M., Blank-Landeshammer, B., Reymond, C.E., Kollipara, L., Sickmann, A., Kucera, M., Westphal, H., 2018. Disentangling thermal stress responses in a reef-calcifier and its photosymbionts by shotgun proteomics. Sci. Rep. 8, 3524. https://doi.org/10.1038/s41598-018-21536-4.

Tanaka, Y., Minggat, E., Roseli, W., 2021. The impact of tropical land-use change on downstream riverine and estuarine water properties and biogeochemical cycles: a review. Ecol. Process. 10, 1–21. https://doi.org/10.1186/s13717-021-00332-3.

Venturelli, R.A., Rathburn, A.E., Burkett, A.M., Ziebis, W., 2018. Epifaunal foraminifera in an infaunal world: insights into the influence of heterogeneity on the benthic ecology of oxygen-poor, deep-sea habitats. Front. Mar. Sci. 5, 344. https://doi.org/10.3389/fmars.2018.00344.

Wickham, H., 2023. ggplot2: Elegant Graphics for Data Analysis, third ed. Springer, New York. Available at: https://ggplot2.tidyverse.org. (Accessed 6 November 2024).

Wickham, H., 2024. reshape2: flexibly reshape data: a reboot of the reshape package. R package version 1.4.4.

Wickham, H., Bryan, J., 2023. Readxl: read excel files. R package. Available at: https://readxl.tidyverse.org. (Accessed 6 November 2024).

Yanko-Hombach, V., Kondariuk, T., Motnenko, I., 2017. Benthic foraminifera indicate environmental stress from river discharge to marine ecosystems: example from the Black Sea. J. Foraminifer. Res. 47, 70–92. https://doi.org/10.2113/gsjfr.47.1.70.